University of Tor Vergata

Consiglio Nazionale delle Ricerche

UNIVERSITY OF ROME "TOR VERGATA"

Dr. Alessandra Di Blasi

PhD Course in "Materials for Environment and Energy"

(XIX cycle)

Low Temperature DMFCs for Portable Applications

Tutor

Dr. Vincenzo Antonucci

Coordinator

Prof. Enrico Traversa

TABLE OF CONTENTS

SUMMARY

Technological improvements in direct methanol fuel cells (DMFCs) are promoted by their exciting perspectives of application in portable, transportation and stationary devices. Direct Methanol Fuel Cells were in the past mainly designed for relatively high temperature (>90°C) operation in order to enhance the methanol electro-oxidation kinetics and to increase the ionic conductivity of the polymeric membrane. New composite membranes have been developed to further extend the operating temperature up to 150°C. High operating temperatures are especially favourable for transportation applications. However, the most promising short term application of DMFC appears now to involve the field of portable power sources[1-4] where they can suitably to replace or support batteries. In this regard, increasing interest is devoted towards the miniaturisation of these fuel cell devices in order to replace the current Li-ion batteries. Theoretically, methanol has a superior specific energy density (6000 Wh/kg) in comparison with the best rechargeable battery, lithium polymer and lithium ion polymer (600 Wh/kg) systems. This advantage translates into much longer conversation times using mobile phones, longer time of continuous operation for laptop computers and more power available on these devices to support consumer demand. In relation to consumer convenience, another significant advantage of the DMFC over the rechargeable battery is its potential for instantaneous refuelling. Unlike rechargeable batteries that require hours for charging a depleted power pack, a DMFC can have its fuel replaced in minutes. These significant advantages make DMFC a promising device in the portable electronic market [5-7].

The research activity of this thesis is addressed towards the development of low temperature (30-60°C) DMFCs for portable applications. The different working conditions of portable system i.e. passive operation mode, air breathing etc., introduce new issues with respect to DMFCs operating at high temperatures; thus development of a system for portable applications requires further efforts.

In this thesis, three fundamental aspects have been mainly addressed, these are:

I. Pt loading: analysis of the influence of the Pt loading on the electrochemical behaviour of a DMFC;

II. Methanol tolerant cathode catalysts: analysis of the catalytic activity for the oxygen reduction reaction in DMFC for Pt alloy with transition metals;

III. Water management: optimization of electrode properties;

IV. Passive mode operation.

The aim of the present work is to contribute to the comprehension of the main issues associated to the low DMFC operation temperature. Such an investigation was carried out by using both physico-chemical and electrochemical methods. Specific tests were carried out by using diagnostic techniques in order to individuate potential solutions to drawbacks affecting DMFCs.

CHAPTER I

PRELIMINARY REMARKS

I.1 INTRODUCTION TO FUEL CELL SYSTEM

Most of the world energy requirements are presently addressed by burning fossil fuel in low efficiency thermal processes. An increasing use of renewable energy sources is necessary to reduce environmental issues such as atmospheric pollution, global warming, green house effect. Besides, renewable energy sources, alternative energy conversion technologies with high efficiency are required. Fuel cells represent a potential solution both in stationary and transportation applications due to their low environmental impact and high conversion efficiency. Fuel cells do not utilize a thermodynamic cycle as opposite of internal combustion engine (ICE). In fact, they convert the chemical energy of a reaction directly into electrical energy. The basic physical structure or building block of a fuel cell consists of an electrolyte layer in contact with a porous anode and cathode on each side. The electrolyte is an ion exchange membrane (fluorinated sulfonic acid polymer or other similar polymers) that is an excellent proton conductor. The typical protonic membrane, e.g. Nafion, plays both the role of an acid medium and of separator between the two electrode compartments. The electrons liberated at the anode by the oxidation of methanol circulate in the external electrical circuit, producing electrical energy, and reach the cathode where they reduce the oxidant, usually oxygen from air. Thus, in a fuel cell there is no direct contact between fuel and oxidant. Therefore, the overall reaction corresponds to the catalytic combustion of the fuel with oxygen.

As well known, the thermal efficiency of a practical machine is always less than 100%. The internal combustion engine efficiency is about 18%, while the typical efficiency of most fuel cells is about 40%. The energy balance of a fuel cell is based on the input chemical and output electrical energy and heat. The energy balance varies for the different types of cells because of the difference in reactions that occur and the operating temperature. In general, the cell energy balance states that the enthalpy flow of the reactants entering the cell will equal to the enthalpy flow of the products leaving the cell plus the sum of four terms: 1) the net heat generated by physical and chemical processes within the cell, 2) the dc power output from the cell, 3) the rate of heat loss from the cell

to its surroundings, 4) the energy required by the auxiliaries e.g. pumps, blowers, compressors.

The ideal thermal efficiency of an energy conversion device defined as the ratio of the amount of useful energy that, in the ideal case of a fuel cell, is the change in Gibbs free energy of a reaction to the enthalpy (ΔH) of the reaction. Thus, the thermal efficiency of an ideal fuel cell operating reversibly on a specific fuel and oxygen at standard conditions is:

$$h_{ideal} = \frac{\Delta G}{\Delta H} \tag{1}$$

Whereas, the thermal efficiency of an actual fuel cell, operating at a cell voltage (V_{cell}), is given by:

$$h = \frac{\Delta G}{\Delta H} * \frac{\Delta E}{\Delta E_{\circ}} * h_f * h_{aux} \quad \rightarrow \quad \frac{\Delta E}{\Delta E_{\circ}} = h_{electricalefficincy} \tag{2}$$

$$h = h_{ideal} * h_{electricalefficincy} * h_f * h_{aux} \tag{3}$$

Fuel utilization, h_f, takes into account the excess of fuel fed to the cell with respect to the stoichiometry amount required to achieve the operating current (Faraday Law). Since in the DMFC, a significant part of fuel is lost in the cross-over process (I_{eq}), the fuel efficiency is defined as:

$$h_f = \frac{I}{I_{eq} + I} \tag{4}$$

h_{aux} refers to the power consumption of the auxiliaries.

In the power consumed by auxiliaries (blower, pumps, ect.) is not negligible, it must be also taken into account in the evaluation of efficiency.

$$h_{aux} = \frac{netW_{electricalpowerout}}{W_{electricalpowerinpuforauxiliary} + netW_{electricalpowerout}} = \frac{netW_{electricalpowerout}}{W_{electricalpowerproduced}} \tag{5}$$

Fuel cells result more advantageous both in terms of fuel utilization and lower environmental impact than ICE:

- H_2-based FCs avoid air pollution coming from fossil fuel combustion;
- FCs do not utilize sulphur containing fuel;
- FCs, working at low temperatures, do not release NO_x into the atmosphere.

However, there are significant difficulties for market application; this is due to both high costs of materials used in fabricating (noble metal catalysts, perfluosulfonic membranes) and the cost of hardware manufacturing (MEAs) which are presently higher than conventional energy conversion system.

Fuel cells include different kind of devices having different working conditions and final applications. They can be classified by use of diverse categories, depending on the combination of type of fuel and oxidant (H_2, CH_3OH, CH_4 ect.), whether the fuel is processed outside (external reforming) or inside (internal reforming) the fuel cell, the type of electrolyte, the temperature of operation, whether the reactants are fed to the cell by internal or external manifolds, etc. The most common classification of fuel cells is by the type of *electrolyte* used in the cells and includes 1) alkaline fuel cell (AFC), 2) phosphoric acid fuel cell (PAFC), 3) molten carbonate fuel cell (MCFC), 4) intermediate temperature solid oxide fuel cell (ITSOFC), and 5) tubular solid oxide fuel cell (TSOFC) and polymer electrolyte fuel cell (PEFC). These fuel cells are listed in the order of approximate operating temperature, ranging from ~100°C for AFC, ~200°C for PAFC, ~650°C for MCFC, ~800°C for ITSOFC, 1000°C for TSOFC and ~80- 130°C for polymer electrolyte fuel cell (PEFC). The operating temperature and useful life of a fuel cell are determined by the physicochemical and thermo-mechanical properties of materials used in the cell components (i.e., electrodes, electrolyte, interconnect, current collector, etc.).

I.2 FUNDAMENTAL ASPECTS

I.2.1 INTRODUCTION TO DMFCS

Direct Methanol Fuel Cells (DMFCs) are promising power sources for a range of applications including transportation, portable power sources and distributed generation of clean energy. For the methanol reaction the overall reaction corresponds to the catalytic combustion of methanol with oxygen.

Thernodynamics of direct methanol fuel cell:

Anode reaction: $CH_3OH + H_2O \rightarrow CO_2 + 6\,H^+ + 6\,e^-$ (6)

cathode reaction: $3/2O_2 + 6e^- + 6\,H^+ \rightarrow 3\,H_2O$ (7)

Overall reaction: $CH_3OH + 3/2\,O_2 \rightarrow CO_2 + 2\,H_2O$ (8)

The free energy and the electromotive force associated with the overal reaction at 25°C and 1 atm are:

$\Delta G_{CH3OH} = -686 kJmol^{-1}$; $\Delta V_{CH3OH} = 1.18V$

The thermal efficiency of an ideal fuel cell, operating reversibly on methanol and oxygen at standard condition, is given by:

$$h_{ideal} = \frac{\Delta G_{CH3OH}}{\Delta H_{form}} \tag{9}$$

where:

$$\Delta H_{formCH3OH} = \Delta H_{prod} - \Delta H_{reag} = 724.3 kJmol^{-1} \tag{10}$$

$$h_{ideal} = \frac{-686 kJmol^{-1}}{-724.3 kJmol^{-1}} = 0.947 \tag{11}$$

I.2.2 DMFC PERFORMANCE

Methanol is an attractive fuel because it is a liquid under atmospheric conditions, hence its storage and transportation is less complicated than hydrogen, and it could be supplied through the existing gasoline infrastructure. Despite of these advantages, major obstacles to their commercial application are:

- slow methanol electro-oxidation and oxygen reduction on the electrodes surface and the complicate diffusion processes of the reactants/products;
- dehydration of the electrolyte working at temperature higher than 120°C;
- water flooding due to the liquid fed to anode side. If there is too much humidification the electrode floods which causes problems with mass transport of the gas to the electrode;
- cross-over of methanol through the electrolyte membrane from the anode to the cathode;
- poisoning of the cathode surface in the presence of methanol cross-over.

Methanol cross-over is an issue that affects cathode performance [8]. Wang et al. [9] found that methanol is oxidized heterogeneously in the presence of oxygen and suitable catalyst leading to a so-called “mixed potential” effect, and that the cathode is additionally poisoned by methanol. The impact of methanol cross-over on the current-voltage-characteristics of prototype DMFCs was investigated in numerous studies [10,11,12,13].

Two options exist to overcome cathode performance losses due to methanol cross-over: i) polymer electrolyte membranes have to be used which allow less methanol permeation, or ii) a cathode catalyst, which neither promotes heterogeneous oxidation of methanol nor methanol poisoning, has to be found [14]. These drawbacks affect cell performance as it is possible to observe in the following scheme, applicable to all fuel cells:

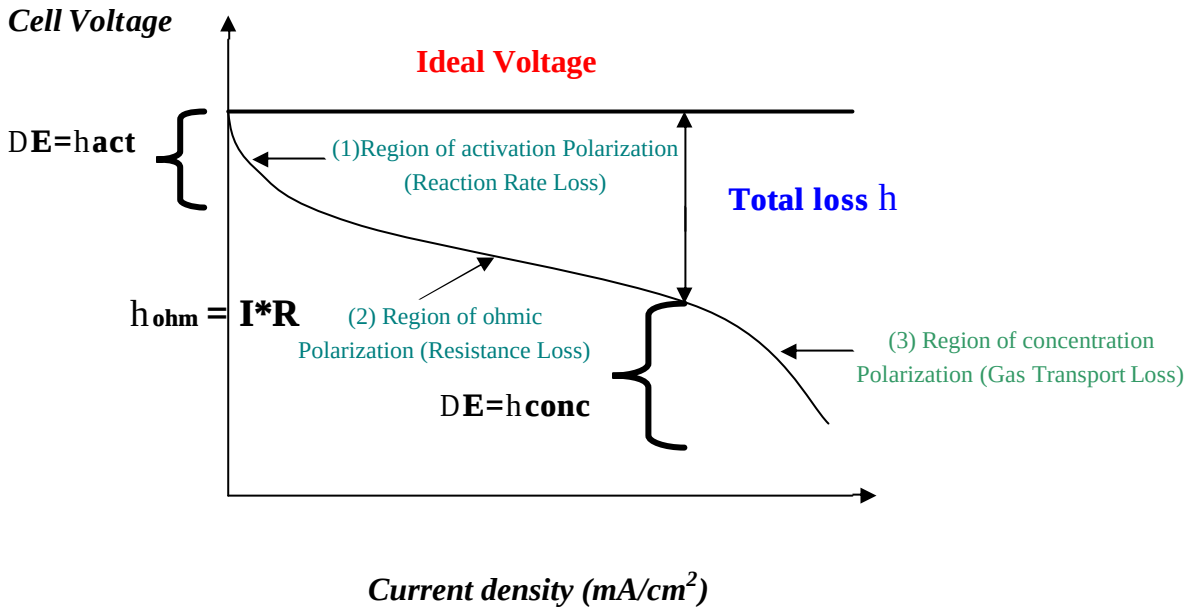

Fig. I-1 Ideal and actual fuel cell voltage/current characteristic

Useful work is obtained ($\Delta G = -nFE$) from fuel cell a reasonable current is drawn, but the actual cell potential is decreased from its equilibrium potential because of irreversible losses, as shown in Figure 1. The losses, which are called polarization, overpotential or over-voltage (η), originate primarily from three sources: (1) activation polarization (act), (2) ohmic polarization (ohm), and (3) concentration polarization (conc) [15]. These losses result in a cell voltage (V) less than the ideal potential, E ($V = E - Losses$).

Activation polarization: activation polarization is present when the rate of an electrochemical reaction at an electrode surface is controlled by sluggish electrode kinetics.

It is possible to study the catalytic activity in this region since a concentration gradient ($C_s = C_b$). In other words, this region is directly related to the rates of electrochemical reactions. Thus, reactants have to overcome an activation barrier.

Current density represents the reaction rate, a small current is associated to a slow reaction rate of methanol oxidized to CO_2. A part of the methanol that does not react will pass through the membrane reaching the cathode compartment, where a mixed potential

will form in the presence of oxygen. The activation polarization can be described by the Tafel equation:

$$\Delta E = \eta_{act} = (RT/\alpha nF) \ln (i/i_o) \quad (12)$$

or

$$\eta_{act} = a + b \log i \quad (13)$$

Where

$a = -2.3RT/\alpha nF \log i_0$

$b = -2.3RT/\alpha nF$

i_0 is an important kinetic characteristic of an electron transfer process, called exchange current density.

Ohmic polarization: the resistance to flow of ions in the electrolyte and resistance to flow of electrons through the electrode materials determine ohmic losses. The dominant ohmic losses, through the electrolyte, are reduced by decreasing the electrode separation and enhancing the ionic conductivity of the electrolyte. Because both the electrolyte and fuel cell electrodes obey to Ohm's law, the ohmic losses can be expressed by the equation:

$$\eta_{ohm} = I * R$$

Concentration polarization: when the reaction is running the reactants react immediately on the electrodes surface ($C_s = 0$). It is important to have a good diffusion rate of the reactants on the catalyst pores and, a good diffusion rate of the products from internal pores. Otherwise, a significant concentration gradient will form, whit $C_s < C_b$.

The reaction rate in this case will be a function of reactants/products flow from reaction sites. There is an inside and outside diffusional control.

This concentration gradient causes an over potential or a potential drop (ΔE) that is recorded as a potential drop:

$$\Delta E = \eta_{conc} = RT/nF \ln (C_s/C_b) \quad (14)$$

If

$$C_s = C_b \rightarrow \eta_{conc} = 0 \quad (15)$$

$$C_s/C_b = (1 - i/i_l) \quad (16)$$

$$\Delta E = \eta_{conc} = RT/nF \ln 1 - i/i_l \quad (17)$$

Where **i** and i_l are the net current density and the limiting current density, respectively.

These losses have to be subtracted from the ideal potential (E):

$$\mathbf{V_{eff} = E_c - E_a - h_{act} - h_c - IR} \quad (18)$$

where

V_{eff} = effective cell potential.

All these aspects lead to a low efficiency and reduced power density performance especially for a DMFC. Thus, the main objectives for Direct Methanol Fuel Cell are:

- to decrease the over voltages and hence to increase the reaction rate both at the anode and at the cathode;
- to increase the reaction selectivity towards complete oxidation to CO_2;
- to find methanol tolerant oxygen cathodes;
- to decrease the effects of methanol cross-over through the ionic membrane by developing advanced membranes with optimum structures and compositions.

I.2.3 STRUCTURAL EFFECTS AND ELECTRODE-KINETICS

The electrocatalytic oxidation of methanol has been thoroughly investigated during the last three decades, particularly in regard to the possible development of DMFCs [16-19]. The oxidation of methanol (the electrocatalytic reaction) is constituted of several steps, which involve adsorbed species. From a general point of view, almost all electro-oxidation reactions involving low molecular weight organic molecules, such as CO, CH_3OH, C_2H_5OH, HCOOH and HCHO, are enhanced by the presence of a Pt-based catalyst [20-23] at least in acidic environment. Determination of the mechanisms for this reaction needs specific information on:

1. the electrode kinetics for the formation of partially oxidized products;
2. the nature and the distribution of adsorbed intermediates at the electrode surface.

The quantitative analyses of reaction products, due to partial or complete oxidation, can be performed by different methods. Apart from a decrease in the Coulombic efficiency, the formation of partially oxidized products can be deleterious for the DMFC application, because some of these may act as poisoning species for the electrode.

The mechanism, by which such synergistic promotion of the methanol oxidation reaction brought about, has been the subject of numerous studies during the last 30-40

years, in which various spectroscopic methods have been employed in conjuction with electrochemistry [6-10]. A combination of cyclic voltammetry [24-29], in situ ellipsometry [30], X-ray absorption spectroscopy [31], on-line mass spectrometry and in-situ FTIR spectroscopic studies [32-37], revealed that the electro-oxidation of methanol on Pt-based catalysts proceeds through the mechanism (sequence of non-elementary reaction steps) below described. First a sequence of dehydrogenation steps give rise to adsorbed methanolic residues, according to the following scheme:

$$Pt + CH_3OH \rightarrow Pt\text{-}(\bullet CH_3OH) \quad (19)$$

$$Pt\text{-}(\bullet CH_3OH) \rightarrow Pt\text{-}(\bullet CH_2OH)_{ads} + H^+ + e^- \quad (20)$$

$$Pt\text{-}(\bullet CH_2OH)_{ads} \rightarrow Pt\text{-}(\bullet CHOH)_{ads} + H^+ + e^- \quad (21)$$

$$Pt\text{-}(\bullet CHOH)_{ads} \rightarrow Pt\text{-}(\bullet CHO)_{ads} + H^+ + e^- \quad (22)$$

Formyl like species $(\bullet CHO)_{ads}$ has been identied, by IR (absorption band at around 1690 cm^{-1}) [38]. After the reaction (22), the formyl like species is spontaneously dissociated on platinum according to the reaction;

$$Pt\text{-}(\bullet CHO)_{ads} \rightarrow Pt\text{-}(\bullet CO)_{ads} + H_{aq}^{+} + e^- \quad (23)$$

The strongly adsorbed CO species was identified as the main poisonig species blocking the electrode active sites for further adsorption of intermediates formed during methanol oxidation [39].

Reaction represented by Eq. (23) is a rather fast process and it is the main reason for the CO poisoning of platinum surface. The configuration of the adsorbed CO species depends on the electrode coverage and on the electrode structure. On a smooth platinum polycrystalline electrode, linearly-bonded CO is the main species at intermediate to high coverage, wherease bridge and multibonded CO are clearly seen at low coverage. Linearly-bond CO is the main species adsorbed on Pt (110), wherease multibonded CO is mainly formed on Pt (111) [40].

The vital step in the reaction mechanism appears to be the formation of the intermediate $(\bullet CHO)_{ads}$, which facilitates the overall reaction. The kinetics of its further desorption and/or oxidation into reaction products are the key steps of the mechanism, leading to complete oxidation. An alternative path to the spontaneous formation of the

poisoning species (Eq. 23), is its oxidation with OH species arising from the dissociation of water according to the following reactions:

$$Pt + H_2O \rightarrow Pt(OH)_{ads} + H^+ + e^- \quad (24)$$

The final step is the reaction of Pt-OH groups with neighbouring methanolic residues to give carbon dioxide:

$$Pt\text{-}CO + Pt(OH)_{ads} \rightarrow 2Pt + CO_2 + H^+ + e^- \quad (25)$$

The overall oxidation process of methanol to carbon dioxide proceeds through a six electron donation process; yet, the rate determining step, derived from electrochemical steady-state measurements on Pt, through analysis of the Tafel slope, involves a one-electron step [32]. On a pure Pt surface, the dissociative chemisorption of water on Pt is the rate determining step at potentials below ≈ 0.7 V vs. RHE, i.e. in the potential region that is of technical interest [32]. It is generally accepted that an active catalyst for methanol oxidation should give rise to water displacement at low potentials and to "labile" CO chemisorption. Moreover, a good catalyst for methanol oxidation should also catalyze the oxidation of carbon monoxide.

I.2.4 Pt-Ru BINARY ALLOY ELECTROCATALYSTS

An alternative approach is to add a second component (a “promoter”) to platinum in order to decrease the formation of poisoning species or to promote their oxidation at lower potential. Even if various theories have been put forward to explain the promoting effect of the additional elements (e.g. Ru, Sn, etc.) [29, 41, 42, 43], this subject remains controversial. Transition metal promoters and adatoms are seen as a means to improve the electrocatalytic behaviour of electrodes, either by minimizing the poisoning reaction or enhancing the main oxidation reaction.

Since the CO oxidation process needs the presence of oxygenated species, numerous types of components have been explored, to generate O or OH species at lower potentials on the platinum surface. Historically, systematic screening of the possible metals show that only a few metals led to a positive results [41]. Ruthenium, tin, molybdenum were carried out to determine the effects of alloying platinum with transition metals groups 4 to 6 on the ease of formation of OH adsorbed species[42]. Despite considerable efforts made over the last twenty years, the best alloying component known to enhance the electro-oxidation

of methanol on platinum is ruthenium. By comparison with the mechanism discussed for pure platinum, the promoting effect of ruthenium can result from a bifunctional mechanism as follows. The adsorbed OH are formed both at Pt sites (reaction (24)), and at Ru sites in a lower potential range. At suitable electrode potentials (0.2 V vs. RHE), water discharging occurs on Ru sites with formation of Ru-OH groups at the catalyst surface. [32]:

$$Ru + H_2O \rightarrow Ru\text{-}(OH)_{ad} + H_{aq}^{+} + e^{-} \quad (26)$$

Then, the oxidation of formyl like species can occur either by (25) or by:

$$Pt\text{-}CO + Ru\text{-}(OH)_{ad} \rightarrow Pt + Ru + CO_2 + H_{aq}^{+} + e^{-} \quad (27)$$

The reaction rate (27) is faster than (25), mainly at lower potentials. According to the mechanism shown above it is generally accepted that Pt sites in Pt-Ru alloys are especially involved in both the methanol dehydrogenation step and the strong chemisorption of methanol residues. Despite considerable research efforts, Pt-Ru alloy are the only acceptable catalyst for the electro-oxidation of methanol at low anode potential.

I.2.5 EXPERIMENTAL METHODS

Many modern instrumental tools of analytical chemistry are already well established in fuel cell-related electrochemistry. These include various programmed potential or programmed current electrochemical methods, in situ FTIR, ellipsometry and differential electrochemical mass spectrometry (DEMS).

Methods employing X-ray radiation have proved to be invaluable for the characterization of technical catalysts —either supported or unsupported—and complete fuel cell electrodes.

X-ray diffraction (XRD) and X-ray photo electron spectroscopy (XPS) are the most frequently used techniques. Alone or in combination with other methods, such as voltammetry and chemisorption, important information about some characteristics of the catalyst can be derived. These include crystallinity, crystallite size, composition, oxidation state of species and possible interactions of the catalyst with the substrate. Extended X-ray absorption fine structure (EXAFS) has been used for the characterization of alloyed fuel cell electrocatalysts [44] and should be extremely useful in methanol anode research because small structural changes could be detected [45]. Fourier transform infrared spectroscopy (FTIR) [46] is among the methods being less common for the

characterization of dispersed catalysts and supports. Transmission electron microscopy (TEM) [47-50] can give information about particle size, surface area and shape of the metal crystallites, while FTIR is able to give an idea about the nature of the surface groups of carbon supports and on the structure of adsorbate species adsorbed on noble metal clusters. Electrochemical impedance spectroscopy (EIS) is also commonly employed with porous electrodes and can provide valuable geometric and kinetic information, especially on cathode properties.

In the late eighties and early nineties, there had been some attempts [51–53] using gas chromatography (GC) in order to carry out the analysis of fuel cell reaction products, that is another critical issue. Unfortunately, GC is far from ideal for this purpose. The time needed for one measurement using gas chromatography is typically of the order of a few minutes. This measuring time, in effect, precludes virtually any real-time monitoring of the formation of fuel cell reaction products. Thus, only discontinuous measurements could be done without the ability to record fast changes of product formation, as being, for instance, likely to occur during voltammetry or potential step techniques.

Even though not directly a part of electrochemistry, the characterization of solid polymer electrolytes (SPEs) is nevertheless an important issue for fuel cell research. Consequently, a view of some important methods available for that purpose should be within the scope of this review article. Basically, the membrane electrolyte has to serve three purposes in a DMFC.

1. It has to provide a high proton conductivity;
2. it needs to have a low permeability for methanol;
3. it has to be stable under the operating temperatures employed.

NMR-spectroscopy in its various forms is certainly an important tool. Nafion®, a perfluorosulfonic acid ionomer, has been found of most significant interest so far with one contribution concerning polybenzimidazole (PBI), a novel SPE, which has been investigated by means of solid-state NMR [54]. NMR-spectroscopy has the advantage that species (e.g. water) sorbed inside the SPE membrane, which frequently provide the pathway for protonic conductivity, can be studied without interference from the polymer matrix.

Another issue concerning SPEs, is thermal stability in cases where long-term operation at elevated temperatures is desired. The various techniques of thermometry are the methods of choice for that purpose. TGA:MS [55,56] and TGA:FTIR [57] are the most

elegant of these methods. Using these two methods, it is not only possible to determine the onset temperature of thermal decomposition, but also some information about the decomposition mechanisms can be extracted at the same time by identifying the decomposition products. However, investigators should be cautioned not to apply the results of thermometric methods carelessly to the problem of long-term stability. Table 1 contains a listing about advantages and disadvantages of the methods discussed.

Table I - 1 Summary of techniques used for general electrochemical catalysis research and for the characterization of fuel cell components

(Reproduced from: "S. Wasmus, A. Kuver / *J. of Electroanalitycal Chemstry* 461 (1999) 14-31)

Technique	*Subject of investigation*	*Advantages*	*Disadvantages*
In-situ FTR	Products and adsorbed species formed at smooth electrodes	• Detection of volatile and non-volatile products • Identification of adsorbed species	Restriction to smooth electrodes with sufficient reflectivity and to liquid electrolytes
Differential electrochemical Mass Spectroscopy (DEMS)	Volatile products formed at sputtered, lacquer-type and technical electrodes	Detention of volatile products using galvanostatic, potentiostatic and potentials weep methods	
X-ray radiation methods (XRD, XPS and EXAFS)	Characterization of technical electrodes	• Qualitative and quantitative analysis of catalyst or support surface composition • Different elements can be studied separately from each other	Quantitative analysis needs careful calibration Sensitivity to contamination
Transmission Electron Microscopy	Characterization of technical electrodes	Determination of particle size and shape	Substrate must be electronically conductive
FTIR	Characterization of technical electrodes	Nature of surface group can be determined	
Electrochemical Impedance Spectroscopy	Characterization of technical electrodes	Electrode structure and kinetic parameter can be determined	Equilibrium conditions are required
NMR spectroscopy	Polimer electrolytes	• Reactions whitin the polimer matrix can be studied • Identify and behavior of sorbed species can be investigated	Sample preparation is critical for reproducible results
Thermogravimetric analysis **TGA, TGA/MS and TGA/FTIR**	Polimer electrolytes	Thermal stability of polymer electrolytes can be assessed	Care has be exercised for applying the results of TGA measurements to long term stability

I. 3 MORPHOLOGICAL ASPECTS OF ELECTROCATALYSTS

I.3.1 ROLE OF SURFACE AREA AND METAL LOADING

As discussed above, the main requirement for an optimal alloy electrocatalyst, such as Pt-Ru, is the synthesis of highly dispersed metal particles on a carbon support. The mass activity (A/g Pt) of the catalyst for methanol electro-oxidation is strictly related to the degree of dispersion, since the reaction rate is generally proportional to its active surface area. In the case of an oxygen reduction electrocatalyst, it was found, after analysing a wide range of Pt and Pt alloy electrocatalysts, that there is an optimum particle size for the metallic phase (about 30 Å), which corresponds to a significantly high mass activity [57]. For this reaction it was found that the specific activity (mA cm^{-2} real surface area) increases with the particle size, but simultaneously decreases with the active surface area. The best compromise was achieved at about 30 Å Pt particle size [57].

In the case of methanol electro-oxidation on carbon supported Pt electrocatalyst, two different trends were observed. Mc Nicol et al. [58] observed for their Pt electrocatalysts a maximum activity at about 80 m^2/g surface area. Recently, another group has shown that the specific activity increases as a function of particle size [59]. Thus, a maximum in mass activity vs. particle size should be observed as in the case of oxygen reduction. On the other hand, Watanabe et al. [60] found that the specific activity for methanol oxidation on a carbon supported Pt electrocatalyst does not change for a particle size above 20 Å (Pt fcc structure); thus, the mass activity increases as the dispersion of the metal phase is increased [60]. These findings have been in part confirmed for the Pt-Ru system for a particle sizes above 30 Å [61]. Not much work has been carried out on electrocatalysts with particle sizes below 20 Å or catalyst formed by an amorphous phase. Generally, most of the Pt-Ru fuel cell electrocatalysts have particle sizes above 20 Å, which are crystalline with a face centred cubic (fcc) structure. Below 20 Å, the distinction between amorphous and crystalline is not so evident. For particles with 10-15 Å size about 50% of the atoms are on the surface and thus there is no ordered structure. Some recent kinetic investigations by Wieckoski et al. [62,63] on Pt surfaces covered with Ru ad-atoms have shown that the surface composed by the (111) Pt crystallographic plane covered by Ru ad-atoms performs better than any other Pt/Ru ad-atoms crystallographic plane. Thus extending these considerations to high surface area Pt-Ru electrocatalysts, the specific activity should increase with the particle size. In fact, a large-size particle possess a high

surface content of (111) planes [57]. Accordingly, a maximum in the electrocatalytic activity should be observed as a function of particle size. Data shown by Ren et al. [58] may be fitted as well with a "volcano" relationship with maximum at 3 nm and shape similar to that generally observed for oxygen reduction. Unfortunately, the scattering due to a variable composition of the Pt-Ru surface, in high surface area electrocatalysts, does not allow to distinguish a clear behaviour. A second aspect concerns the loading of the metal phase on the carbon support. A high weight percent (wt%) of Pt on the carbon substrate will significantly decrease the anode thickness for the same Pt loading per geometric electrode area (e.g., 1 mg cm^{-2}). Using this approach, it will be possible to enhance mass transport through the electrode and simultaneously reduce the ohmic drop. However, it has been found that an increase of the Pt loading (above 40 wt.%) on the carbon support decreases the dispersion of the electrocatalyst, probably due to some particle agglomeration.

I.3.2 ROLE OF CARBON SUPPORT

In general preparation procedures, such as impregnation, colloidal deposition, surface reaction involve the adsorption step of active compounds on a carbon black surface. The synthesis of a highly dispersed electrocatalyst phase in conjuction with a high metal loading on carbon support has been one of the goals of the recent activity in the field of DMFCs. In this regard it is of interest to determine which carbon black is the most suitable as the support. In recent reports [64- 66], the mostly used carbon blacks were: Acetylene Black (BET Area: 50 m^2/g), Vulcan XC-72 (BET Area: 250 m^2/g) and KETJEN Black (BET Area: 1000 m^2/g).

All these materials have optimal electronic conductivity but, as denoted above, they differ for the BET surface area and thus very probably in the morphology. A low surface area carbon black (such as Acetylene Black) will not allow high dispersion of the metal phase, especially for a high metal loading (low carbon content); on the other hand, it does not have micropores in the structure, which could hinder mass transport through the electrocatalytic layer. A high surface area carbon black can easily accommodate a high amount of metal phase, with a high degree of dispersion but, at the same time, the significant amount of micropores on the carbon support will not allow a homogeneous distribution of the electrocatalytic phase through the support, which could lead to mass transport limitations of the reactant as well as its limited access to the inner electrocatalytic

sites. Vulcan XC appears to be the best compromise with the presence of a small amount of micropores and a reasonable high surface area sufficient to accommodate a high loading of the metal phase. Up to now, this carbon black is the most used carbon support for the preparation of DMFCs catalysts.

I.3.3 PREPARATION METHODS

There are various routes for the synthesis of the Pt-Ru/carbon black electrocatalyst; these can be grouped into two main types, i.e., an impregnation and a colloidal procedure. An impregnation procedure is characterized by an impregnation step of Pt and Ru precursors (e.g., H_2PtCl_6, $RuCl_3$, $Pt(NH_3)_2(OH)_2$, Ru_3CO_{12}, $Pt(NH_3)_2(NO)_2$, etc.) which is followed by a final reduction step. This can be a chemical reduction of the electrocatalyst slurry in aqueous solution by using N_2H_4, NaS_2O_5, NaS_2O_3, $NaBH_4$ (liquid-phase-reduction) or gas-phase reduction of the impregnated carbon black by a flowing hydrogen stream. It has been shown that the impregnation method can be used for the synthesis of a multifunctional system, e.g., from a bimetallic to a quaternary electrocatalyst (Pt-Ru-Sn-W) [67]. However, it requires the use of high surface area carbon black such as Ketjen black whose limitations for the operation of a methanol fuel cell have been pointed out above. Furthermore, this procedure does not allow one to obtain high dispersions in the case of high metal loadings.

There are various colloidal deposition routes, for example, as used by Jalan [68], Bonneman et al. [69], Petrow and Allen [70], etc. The advantages of these preparation routes consist of the attainment of significantly high surface areas in the presence of high metal loading on carbon. The main disadvantages are the presence of some complex preparation steps in the overall synthesis, the use in some cases of organic compounds/solvents and the increase of costs of production. An additional method is based on the thermal decomposition. In this case, unsupported high surface area electrocatalysts are obtained by thermal decomposition of appropriate high molecular weight Pt-precursors such as Pt-carbonyl compounds [71]. Other methods, such as co-precipitation sol-gel or physical methods (e.g., sputtering [72]) have not stimulated much interest in the past, but they are now becoming interesting for the synthesis of catalysts for portable power sources [72]. The choice of the most appropriate preparation procedure relies on the following considerations. It is well known that the preparation procedure of electrocatalysts influences their physico-chemical properties and thus their activities for

methanol oxidation reaction and the oxygen reduction. The performance characteristics of an electrocatalyst depend on its chemical composition (surface and bulk), structure and morphology. Accordingly, the selected methodology of electrocatalyst synthesis should allow one to address the process for the attainment of a proper structure (crystalline or amorphous) and with a chemical composition on the surface as close as possible to the nominal or bulk composition. Since the rate of all electrocatalytic reactions is strictly related to the active surface area besides surface chemistry, the morphology of the electrocatalyst needs to be tailored. Morphology is not only related to the metal-phase area but also to the presence of micro and macro pores in the electrocatalyst support which could facilitate or hinder the mass transport properties. All these characteristics determine the cell performance even if the relative influence of each parameter is still not known in detail. It is thus necessary to select appropriate procedures for an optimization of these characteristics i.e., composition, structure, particle size, porosity etc. Generally a combination of physico-chemical and electrochemical analyses carried out on electrocatalysts with different characteristics indicates the system that better suits the scope of application in a DMFC.

I.4 CATHODIC REDUCTION OF OXYGEN

I.4.1 GENERAL CONSIDERATIONS

Although Pt/C electrocatalysts are, at present, the most widely used materials as cathodes in low temperature fuel cells, due to their intrinsic activities and stabilities in acidic solutions, there is still great enthusiasm to develop more active, selective and less expensive electrocatalysts for oxygen reduction. Since it is widely established that Pt cannot be easily replaced (at least for the moment) by other electrocatalysts for the oxygen reduction reaction (ORR), there are a few directions that can be investigated to reduce the costs and to improve the electrocatalytic activity, especially in the presence of methanol cross-over. One is to increase Pt utilization. This can be achieved either by increasing its dispersion on carbon and the interfacial region with the electrolyte. Another successful approach to enhance the electrocatalysis of O_2 reduction is by alloying of Pt with transition metals. This enhancement in electrocatalytic activity has been differently interpreted, and several studies were made to analyze in depth the surface properties of the proposed alloys combinations [73-77]. Although a comprehensive understanding of the numerous reported evidences has not yet been reached, the observed electrocatalytic

effects have been ascribed to several factors (interatomic spacing, preferred orientation, electronic interactions) which play, under fuel cell conditions, a favourable role in enhancing the oxygen reduction reaction (ORR) rate [78-82]. High specific activities of Pt-Cr and Pt-Cr-Co alloy electrocatalysts for oxygen reduction as compared with that on platinum were observed in H_2-air polymer electrolyte membrane fuel cells (PEMFCs) [73,82]. The formation of a tetragonal ordered structure upon thermal treatment, in the case of Pt-Co-Cr, leads to a more active electrocatalyst than that with a Pt fcc structure [78-82]. Moreover, even in the presence of methanol cross-over, the performance of highly selective electrocatalysts for oxygen reduction would be (in theory) less affected by poisoning phenomena on account of the lower chemisorption energy of methanol on the alloys in comparison with that on Pt. Another goal in this field is to obtain very small sizes for the Pt alloy particles supported on carbon. In the case of Pt-Co-Cr particles with a tetragonal structure, the state of art electrocatalysts have a particle size of 6 nm [78-82]. In addition to the co-precipitation and impregnation methods for preparation of these alloys on a carbon support, colloidal preparation procedures have also been recently investigated [83].

I.4.2 OXYGEN ELECTROREDUCTION IN DMFCS

For the development of cathode electrocatalysts for DMFCs, two main aspects should be taken into account. The electrocatalysts should be very selective for oxygen chemisorption and thus highly active for oxygen electroreduction. In other words, the electrocatalysts should have a composition which will not be poisoned by the methanol cross-over from anode to cathode while maintaining high reaction rates for oxygen reduction. In most cases, a compromise between electrocatalytic activity and resistance to poisoning is necessary. The most widely used electrocatalysts employed in low temperature fuel cells for the oxygen reduction are based on platinum. As discussed in a previous section, various studies conducted in the past, especially on carbon supported Pt electrocatalysts for oxygen reduction in phosphoric acid fuel cells, showed that the electrocatalytic activity (mass activity, mA g^{-1} Pt, and specific activity, mA cm^{-2} Pt) depends on the mean particle size. The mass activity for oxygen reduction reaches a maximum at a mean particle size of 30 Å, corresponding closely to the particle size at which there is a maximum in the fraction of (111) and (100) surface atoms on Pt particles of cubo-octahedral geometry [57]. On the other hand, the specific activity increases

gradually with an increase in the Pt particle size and closely follows the trend observed between the surface fraction of (111) and (100) Pt atoms and the particle size. These results have indicated that the (111) and (100) surface atoms are more electro-catalytically active than Pt atoms located on high Miller index planes [57]. Platinum atoms at edge and corner sites are considered to be less active than Pt atoms on the crystal faces. Accordingly, the mass and specific activity should decrease significantly as the relative fraction of atoms at edge and corner sites approach unity [57]. This situation occurs with Pt particles smaller than 10 Å diameter. Most of the experimental evidence observed in PEMFCs shows that crystalline electrocatalysts with about 25-30 Å particle size have higher activities than amorphous particles and also electrocatalysts with larger crystallite sizes [84].

In the case of DMFCs, an additional aspect should be considered; this is in regard to the methanol cross-over through the membrane. Methanol oxidation and oxygen reduction in the cathode compartment compete for the same sites producing a mixed potential which reduces the cell open circuit potential. In order to better understand these effects, it is worthwhile considering the mechanism for methanol oxidation and oxygen reduction; possible mechanisms are presented below.

Oxygen reduction:

$$O_2 + Pt \rightarrow Pt\text{-}O_2 \quad (28)$$

$$Pt\text{-}O_2 + H^+ + e^- \rightarrow Pt\text{-}HO_2 \quad (29)$$

$$Pt\text{-}HO_2 + Pt \xrightarrow{rds} Pt\text{-}OH + Pt\text{-}O \quad (30)$$

$$Pt\text{-}OH + Pt\text{-}O + 3H^+ + 3e^- \rightarrow 2Pt + 2\,H_2O \quad (31)$$

Equation (30) indicates an intermediate step requiring a dual-site reaction, and if it is the rate-determining step, it is more affected by particle size than intermediate step represented by equation (29). When the particle size becomes very small, then only the inactive edge and corner atoms will be present and dual sites of the proper orientation would not be available. Thus the activity of the particle should be lower. According to the observed variation of the reaction rate with particle size, one may conclude that the rate-determining step is represented by Eq. 12 [83].

Methanol oxidation at the cathode side

$$CH_3OH + 3Pt \rightarrow Pt_3\text{-}COH \quad (32)$$

$$Pt_3COH \rightarrow Pt\text{-}CO + H^+ + 2Pt \quad (33)$$

$$Pt + H_2O \rightarrow Pt\text{-}OH + H^+ + e \quad (34)$$

$$Pt\text{-}OH + PtCO \rightarrow 2Pt + CO_2 \quad (35)$$

In the case of methanol oxidation at the cathode, three neighboring Pt sites in a proper crystallographic arrangement will favour the methanol chemisorption. Since at high cathodic potentials the water discharging reaction (Eq. 34) is largely favored, oxidation of the methanolic residues adsorbed on the surface proceeds very fast producing a parasitic anodic current on this electrode.

When the particle size of the electrocatalyst is very small or one has an amorphous Pt electrocatalyst for the oxygen reduction, methanol chemisorption energy could be lower and hence the cathode less poisonable. But, at the same time, due to the fact that only the inactive edge and corner atoms will be present and dual sites of the proper orientation will not be available, the activity of such electrocatalyst for oxygen reduction will be lower. The best compromise is to modulate the structure and the particle size between amorphous and crystalline in order to decrease the poisoning by methanol and enhance oxygen reduction.

A second possibility is to use a promoting element for oxygen reduction which simultaneously hinders the methanol chemisorption still maintaining the proper structure and particle size.

I.4.3 CARBON SUPPORTED ELECTROCATALYSTS

In order to enhance the resistance to methanol poisoning of the cathode, research activities based on the modification of Pt electrocatalyst by addition of transition metals were recently initiated in various laboratories [83, 85]. In phosphoric acid and PEMFCs the intrinsic electrocatalytic activity of Pt alloys (Pt-Cr, Pt-Ni, Pt-Cr, Pt-Cu, Pt-Fe), with a lattice parameter smaller than that of Pt, is higher than the base metal [73-82]. This effect is related to the nearest neighbour distance of Pt-Pt atoms on the surface of the fcc crystals. Since it has already been observed that the rate determining step involves the rupture of the O-O bond through a dual site mechanism, a decrease of the Pt-Pt distance favours the dual site O_2 adsorption. Most of these evidences are derived from studies

carried out in phosphoric acid fuel cells. In such cases leaching of non-noble elements produces a surface roughening with a corresponding increase of the Pt surface area. A considerably lower number of studies has been carried out on Pt-alloys as electrocatalysts for ORR in PEMFCs [73, 82, 84]. In this case, since the electrolyte anions are chemically bound to the backbone of perfluorosulfonic acid membranes and the cell temperature is relatively low, corrosion problems are minimised compared to phosphoric acid fuel cells. Also in the case of PEMFCs, there is specific evidence for an enhancement of the reaction rate for O_2 reduction on a Pt- alloy electrocatalyst [73, 82, 84]. As pointed out in a previous sub-section, methanol chemisorption and oxygen reduction reactions require an appropriate geometrical arrangement of Pt atoms. Both processes are favoured on a Pt (111) surface, which possesses the reasonable nearest Pt-Pt interatomic distance. Thus, the poisoning effect of methanol cross-over should be more significant on the Pt (111) surface. The lack of information in this field, however, does not allow one to quantify the compensation effect due to the increased methanol oxidation rate at the sites where oxygen reduction is favoured. Beside these aspects, recent work has also taken into consideration the role played by the promoting element (Co, Cr) for the removal of strongly bonded oxygenated species on Pt through an intra-alloy electron transfer [85]. Chemisorption of oxygen molecules occur more easily on oxide-free Pt surfaces [85]. But, as well documented by cyclicvoltammetric analyses [31], methanol adsorption and oxidation are favoured on a reduced Pt surface rather than on platinum oxide. In other words, the addition of Co and Cr to Pt, simultaneously favours the oxygen reduction and methanol oxidation reactions. Furthermore, the presence of electropositive elements, alloyed to Pt, favours the chemisorption of OH species on Pt neighbouring sites. In the absence of oxygen, a small but noticeable promoting effect for methanol oxidation in a wide range of anodic overpotentials has been observed by Cr, Fe and other elements usually selected as catalytic enhancers for the oxygen reduction reaction in PEMFCs [20]. At present, it is difficult to establish if the beneficial effect on oxygen reduction is prevailing with respect to the promoting effect on methanol oxidation at DMFC cathode. In a recent paper, a limited enhancement of ORR was shown when a Pt-alloy instead of Pt was used in DMFCs [83], whereas in other cases, it was observed that Pt-alloys are less tolerant than Pt alone to methanol.

The preparation of cathodic Pt-based electrocatalysts for DMFCs are pratically the same as for the anodic electrocatalysts. However, there are some differences in terms of

the thermal treatment of a Pt-Ru or Pt-Sn alloy for methanol oxidation and that of a Pt-Cr, Pt-Co, Pt-Co-Cr electrocatalysts for oxygen reduction [73-82]. In the latter case, the activation temperature is significantly higher, around 700-900 °C, compared to 100-400°C adopted for the anodic alloy. In the case of the cathode electrocatalyst, a complete alloying is generally accompanied, in most cases, by a phase transition from fcc (cubic) to an ordered tetragonal (fct) structure. This treatment causes an increase of the mean particle size. Thus, the increase of intrinsic electrocatalytic activity is counteracted by the decrease of the surface area of the electrocatalysts.

I.5 *REFERENCES*

[1] M. Neergat, D. Leveratto, U. Stimming, F*uel Cells* 2, 25 (2002).

[2] S. Wasmus and A. Kuver, *J. Electroanal. Chemistry* **1999,** *461*, 14.

[3] A. Blum, T. Duvdvani, M. Philosoph, N. Rudoy, E. Peled, *J. Power Sources* 117, 22 (2003).

[4] T. Yoshitake, H. Kimura, S. Kuroshima, S. Watanabe, Y. Shimakawa, T. Manako, S. Nakamura,, Y. Kubo, *Electrochemistry* 70, 966 (2002).

[5] R. Dillon, S. Srinivasan, A.S. Aricò, V. Antonucci, *J. Power Sources* 127, 112 (2004).

[6] X. Ren, P. Zelenay, S. Thomas, J. Davey, S. Gottesfeld, *J. Power Sources* 127, 112 (2004).

[7] S.C. Kelley, G.A. Deluga, W.H. Smyrl, *Electrochem. Solid-State Lett.* 3, 407 (2000).

[8] M.K. Ravikumar, A.K. Shukla, J. Electrochem. Soc. 143 (1996) 2601.

[9] J.-T. Wang, S. Wasmus, R.Savinell, J Electrochem. Soc. 143 (1996) 1233

[10] A. Kuver, I. Vogel, W. Vielstich, J. power Sources 52 (1994) 77.

[11] A. Kuver, I. Vogel, W. Vielstich, 45th Meeting of the International Society of Electrochemstry, Porto 1994, Abstract OIV-4.

[12] D.L. Maricle, B.L. Murach, L.L. Van Dine, 36th Power Sources Conference, Cherry Hill, NJ, 1994, p. 99.

[13] A. Kuver, W. Vielstich, J. Power Sources 74 (1998) 211-218

[14] K. Sundmacher, O. Nowitzki, U. Hoffman, Chem. Ing.Tech. 69 (1997) 8197.

[15] Fuel Cell Handbook

[16] B. D. McNicol, D. A. J. Rand, *J. Power Sources for Electric Vehicles: studies in electrical and Electronic Engineering*, **1984**, *pp. 807-838.*

[17] C. Lamy, J.-M. Léger, *Proc. 1st International Symposium on New Materials for Fuel Cell System*, Ed. By Savadogo, P.R. Roberge and T.N. Veziroglu, Montreal, 1995, pp. 296-309.

[18] M.P. Hogarth and G.A. Hards, Platinum Metal Rev. 40 (1996) 150.

[19] C. Lamy, J.-M. Léger, *J.Phys. IV, C1, vol. 4 (1994) 253.*

[20] B. D. McNicol, D. A. J. Rand, K. R. Williams, *J. Power Sources* **1999**, *83*, 15.

[21] A. Hamnett, *Catalysis Today* **1997**, *39*, 445.

[22] M. P. Hogarth and G. A. Hards, *Platinum Metal Rev.* **1996**, *40*, 150.

[23] R. Parsons, T. Van der Noot, *J. Electroanal. Chem.* **1988**, *257*, 9.

[24] D. Pletcher and V. Solis, *Electrochim. Acta*, **1982**, 27, 775.[25] K. Wang, H. A. Gasteiger, N.M. Markovic and P. N. Ross Jr., *Electrochim. Acta*, **1996**, *41*, 2587.[26] J. B.

Goodenough, A. Hamnett, B. J. Kennedy, R. Manoharan and S. Weeks, *J. Electroanal. Chem.* **1988**, *240*, 133.

[27] B. Beden, F. Kardigan, C. Lamy, J. M. Leger, *J. Electroanal. Chem*. **1981**, *127*, 75.

[28] K. Chandrasekaran, J. C. Wass, and J. O' M. Bockris, *J. Electrochem. Soc.* **1990**, *137*, 518.

[29] M. Watanabe and S. Motoo, *J. Electroanal. Chem*. **1975**, *60*, 275.

[30] E. Ticianelli, J. G. Berry, M. T. Paffet, and S. Gottesfeld, *J. Electroanal. Chem.* **81**, *229*, 1977.

[31] R. A. Lampitt, L. P .L. Carrette, M. P. Hogarth, A. E. Russell, *J. Electroanal. Chem.* **1999**, *460*, 80.

[32] K. Chandrasekaran, J. C. Wass, and J. O' M. Bockris, *J. Electrochem. Soc.* **1990**, *137*, 518.

[33] J. Clavilier, C. Lamy, and J. M. Leger, *J. Electroanal. Chem*. **1981,** *125*, 249.

[34] P. A. Christensen, A. Hamnett and G. L. Troughton, *J. Electroanal. Chem*. **1993**, *362*, 207.

[35] X. H. Xia, T. Iwasita, F. Ge and W. Vielstich, *Electrochim. Acta* **1996**, *41*, 711.

[36] R. A. Lampitt, L. P .L. Carrette, M. P. Hogarth, A. E. Russell, *J. Electroanal. Chem.* **1999**, *460*, 80.

[37] W. Vielstich, P. A. Christensen, S. A. Weeks and A. Hamnett, *J. Electroanal. Chem.* **1988**, *242*, 327.

[38] B. Beden, F. Hahn, S. Juanto, C. Lamy and J.-M. Legér, *J. Electroanal. Chem.* 225, **1987**, 215.

[39] B. Beden, C. Lamy, A. Bewick and K. Kunimatsu, *J. Electroanal. Chem.* 121, **1981**, 343.

[40] S. Juanto, B. Beden, F. Hahn, J.-M. Legér and C. Lamy, *J. Electroanal. Chem.* 237, **1987**, 119; ibid. 238 (1987) 323.

[41] M. M. P. Janssen, J. Moolhuysen, *Electrochim. Acta* **1976**, *21*, 861.

[42] A. B. Anderson, E. Grantscharova and S. Seong, *J. Electrochem. Soc.* **1996**, *143* , 2075.

[43] J. Mc Breen and S. Mukerjee, *J. Electrochem. Soc.* **1995**, *142*, 3399.

[44] L. Troger, A. Freund, P. Albers, K. Seibold, G. Prescher, Ber. Bunsenges, *Phys. Chem.* 101, **1997**, 851.

[45] P.G. Allen, S.D. Conradson, M.S. Wilson, S. Gottesfeld, I.D. Raistrick, J. Valerio, M. Lovato, *Electrochem. Acta,* 39, **1994**, 2415.

[46] T. Torre, A.S. Aricò, V. Alderucci, V. Antonucci, N. Giordano, *Appl. Catal.* 114, **1994**, 257.

[47] A.S. Aricò, P. Cretì, N. Giordano, V. Antonucci, P.L. Antonucci, A. Chuvilin, *J. Appl. Electrochem.*. 26, **1996**, 959.

[48] A.S. Aricò, P. Cretì, H. Kim, R. Mantenga, N. Giordano, V. Antonucci, *J. Electrochem. Soc., 143*, **1996**, 3838.

[49] M Uchida, Y. Aoyama, N. Tanabe, N. Yanagihara, E. Eda, A. Ohta, *J. Electrochem. Soc.*, 142, **1995**, 2572.

[50] S.C. Roy, P.A. Christensen, A Hamnet, K.M. Thomas, V. Trapp, *J. Electrochem. Soc.*,143, **1996**, 3073.

[51] I. Yamanaka, K. Otsuka, *Electrochim. Acta 34*, **1989**, 211.

[52] H. Nakajima, H. Kita, *Electrochim. Acta* 33, **1988**, 521.

[53] R. Liu, P.S. Fedkiw, *J. Electrochem. Soc.*, 139, **1992**, 3514.

[54] S. Wasmus, R.F. Savinell, H. Moaddel, M.H. Litt, C. Rogers, A. Valeriu, G.D. Mateescu, D.A. Tryk, W.A. Daunch, P.L. Rinaldi, 187th Meeting of the Electrochemical Society, Reno / Nevada, May 21-26 **1995**.

[55] R.S. Samms, S. Wasmus, R.F. Savinell, J. Electrochem. Soc., 143, **1996**, 1225.

[56] B. Gupta, J.G. Highfield, G.G. Scherer, J. Appl. Polym. Sci. 51, **1994**, 1659.

[57] N. Giordano, E. Passalacqua, L. Pino, A. S. Aricò, V. Antonucci, M. Vivaldi and K. Kinoshita, *Electrochimica Acta* **1991**, 36, 1979.

[58] B. D. McNicol, D. A. J. Rand, K. R. Williams, *J. Power Sources* **1999**, *83*, 15.

[59] J. A. Poirier, *The Electrochemical Society Interface*, Winter **1994**, p. 49.

[60] M. Watanabe S. Saegusa, and P. Stonehart, *J. Electroanal. Chem*. **1989**, *271*, 213.

[61] X. Ren, P. Zelenay, S. Thomas, J. Davey, and S. Gottesfeld, *J. Power Sources* **2000**, *86*, 111.

[62] W. Chrzanowski and A. Wieckowski, *Langmuir*, **1998**, *14*, 1967.

[63] H. Kim and A. Wieckowski, Third International Symp. On New Materials for Fuel Cells.

[64] P. S. Kaurenan and E. Skou, *J. Electroanal. Chem*. **1996**, *408*, 189.

[65] M. K. Ravikumar and A. K. Shukla, *J. Electrochem. Soc*. **1996**, *143*, 2601.

[66] J. B. Goodenough, A. Hamnett, B. J. Kennedy, S. A. Weeks, *Electrochim. Acta* **1987**, *32* 1233.

[67] A. S. Aricò, Z. Poltarzewski, H. Kim, A. Morana, N. Giordano and V. Antonucci. *J. Power Sources* **1995**, *55*, 159.

[68] V. Jalan, Extended Abstracts, Electrochemical Society, Los Angeles, CA, Fall Meeting, Abstract 192 (October **1979**).

[69] H. Bonnemann, R. Brinkmann, W. Brijoux, E. Dinjus, T. Joussen, B. Korall, *Angew. Chem.* **1991**, *103*, 1344.

[70] H. G. Petrow and R. J. Allen, *U.S. Pat.* 3, 992, 331, **1976**.

[71] K. Machida, A. Fukuoka, M. Ichikawa and M. Enyo, *J. Electrochem. Soc*., **1991**, *138*, 1958.

[72] C. K. Witham, W. Chun, T. I. Valdez and S. R. Narayanan, *Electrochem. Solid-State Lett.* **2000**, *3*, 497.

[73] S. Mukerjee, S. Srinivasan, *J. Electroanal. Chem*. **1993**, *357*, 201.

[74] T. R. Ralph, G. A. Hards, S. D. Flint, J. M. Gascoyane, Fuel Cell Seminar Abstracts, p. 536, Palm Springs, CA, Nov. 16-19, **1998**.

[75] M. T. Paffet, G. J. Beery, S. Gottesfeld, *J. Electrochem. Soc.* **1998**, *135*, 1431.

[76] M. Watanabe, K. Tsurumi, T. Mizukami, T. Nakamura, P. Stonehart, *J. Electrochem. Soc.* **1994**, *141*, 2659.

[77] A. Freund, J. Lang, T. Lehman, K. A. Starz, *Cat. Today* **1996**, *27*, 279.

[78] V. Jalan, E. J. Taylor, *J. Electrochem. Soc.* **1983**, *130*, 2299.

[79] S. Gottesfeld, M. T. Paffett, A. Redondo, *J. Electroanal. Chem.* **1986**, *205*, 163.

[80] B. C. Beard, P. N. Ross, *J. Electrochem. Soc.* **1970**, *137*, 3368.

[81] K. T. Kim, J. T. Whang, Y. G. Kim, J. S. Chung, *J. Electrochem. Soc.* **1993**, *140*, 31.

[82] S. Mukerjee, S. Srinivasan, M. P. Soriaga, J. McBreen, *J. Electrochem. Soc.* **1995**, *142*, 1409.

[83] M. Neergat, A. K. Shukla, K. S. Gandhi, *J. Appl. Electrochem.* **2001**, *31*, In press.

[84]Y. Takasu, T. Iwazaki, W. Sugimoto and Y. Murakami, *Electrochemistry Communications* **2000**, *2*, 671.

[85] A. S. Aricò, A. K. Shukla, H. Kim, S. Park, M. Min and V. Antonucci, *Appl. Surf. Sci.*

[86] A. Hamnett, *Catalysis Today* **1997**, *39*, 445

CHAPTER II

INFLUENCE OF CATALYST UTILIZATION ON THE ELECTROCHEMICAL BEHAVIOUR OF LOW TEMPERATURE DMFC

II. INTRODUCTION

The increasing demand for quality, energy density, and time-performance of power supply is the principal driving force in the portable power production market. For this application technology, it is necessary to work using catalysts having a high activity at room temperature. In order to reach this goal, the first step of this study was focused on an analysis of the influence of the different Pt loading on the electrochemical behaviour of a DMFC, to get information on catalyst utilization for this application.

II. 1 EXPERIMENTAL

In order to reduce ohmic drop, mass transport and manufacturing problems deriving by the use of thick electrodes, the present DMFC catalysts for low temperature applications are usually unsupported Pt and Pt-Ru alloys [1-3]. Yet, the presence of catalyst agglomeration effects in unsupported catalysts significantly limits their utilisation in polymer electrolyte fuel cell systems. In this work, an 85% Pt-Ru (1:1 a/o) alloy supported on Vulcan XC-72 and a 60% Pt/Vulcan XC-72 were in-house prepared and utilized in DMFCs for the electro-oxidation of methanol and the electrochemical reduction of oxygen, respectively. Both catalysts were in-house prepared by using a sulphite complex route [4]. The preparation procedure involved three main steps: (i) synthesis of the Pt and Ru sulphite precursors, (ii) decomposition of the precursors by H_2O_2 into colloidal amorphous oxides, (iii) gas phase reduction in a hydrogen stream to form metallic phases. A description of the preparation procedure has been reported elsewhere [5]. These carbon supported catalysts associate high metal surface area to a suitable concentration of the active phase that allows to maintain a low electrode thickness.

X-ray diffraction powder (XRD) patterns of the anode and cathode catalysts were obtained on a Philips X'Pert X-ray diffractometer using a CuKα-source. TEM analysis was carried out by a Philips CM12 microscope. The catalysts were intimately mixed with

Nafion ionomer (85 wt% catalyst, 15 wt% Nafion ionomer on a dry basis) by ultrasonic treatment. Pt loadings ranging between 1 and 10 mg cm^{-2} were used for both anode and cathode. A Nafion 117 membrane was used as electrolyte. Membrane-electrode assemblies (MEAs) were formed by a hot-pressing procedure [3] and subsequently installed in a fuel cell test fixture of 5 cm^2 active area. This latter was connected to a test station including an HP6060B electronic load or to an EG&G electrochemical apparatus consisting of a PAR 273A Potentiostat/Galvanostat and a 20A Current Booster.

For single cell polarization experiments, aqueous methanol (1M) was pre-heated at the same temperature of the cell and fed to the anode chamber of the DMFC through a peristaltic pump; dry air, pre-heated at the same temperature of the cell, was fed to the cathode. Atmospheric pressure in the anode and cathode compartments was used in most experiments; whereas, 2 atm rel. was settled at the cathode side in a few experiments to observe the effects of cathode pressure in counteracting methanol cross-over. Reactant flow rates were 2 ml min^{-1} and 350 ml min^{-1} for methanol/water mixture and air stream, respectively. Single cell performances were investigated by steady-state galvanostatic polarization measurement.

II. 2 Results and Discussion

II.2.1 Physico-Chemical Characterization

X-ray diffraction analysis (Fig. II-1) shows the diffraction peaks of the fcc structure typical of Pt and Pt-Ru alloy. Due to the high concentration of noble metals supported on carbon black, only a slight X-ray scattering for graphitic carbon is observed at about $2\theta \cong 25°$. A shift to higher Bragg angles and an increase of peak broadening is observed for the Pt-Ru catalyst with respect to pure Pt, indicating a decrease of lattice parameters and average particle size, respectively. The lattice parameter is about 21 Å for the Pt-Ru alloy catalyst and 37 Å for the Pt catalyst, as calculated by the Sherrer equation.

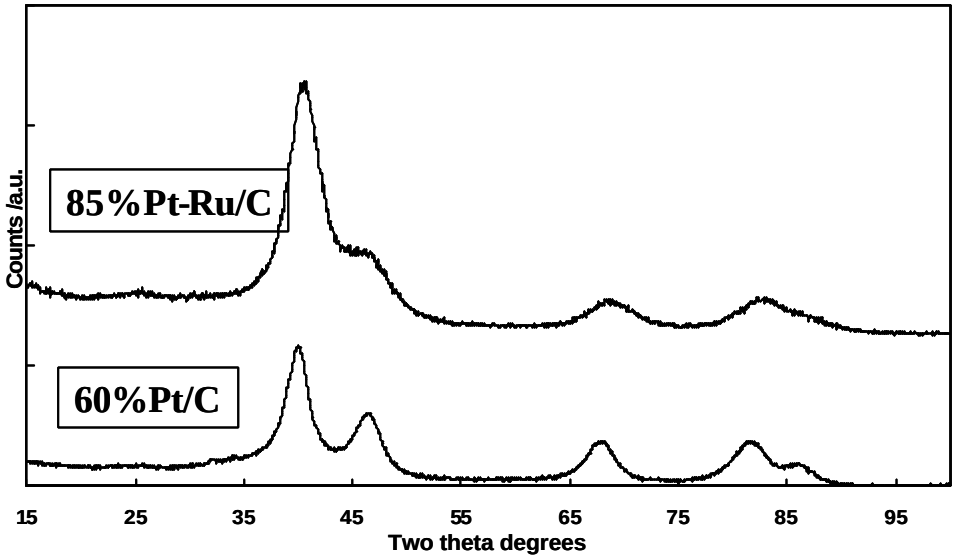

Fig II-1. XRD patterns of 85% Pt-Ru/C and 60% Pt/C catalysts.

TEM observation of the two catalysts (Fig. II-2) shows a good dispersion of the metal particles on the support, even if some particle agglomerations due to the high concentration of metal on carbon support are observed.

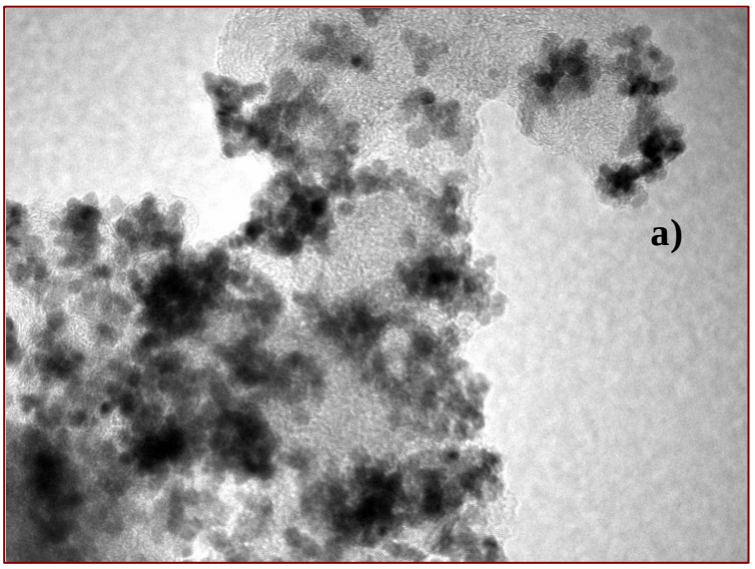

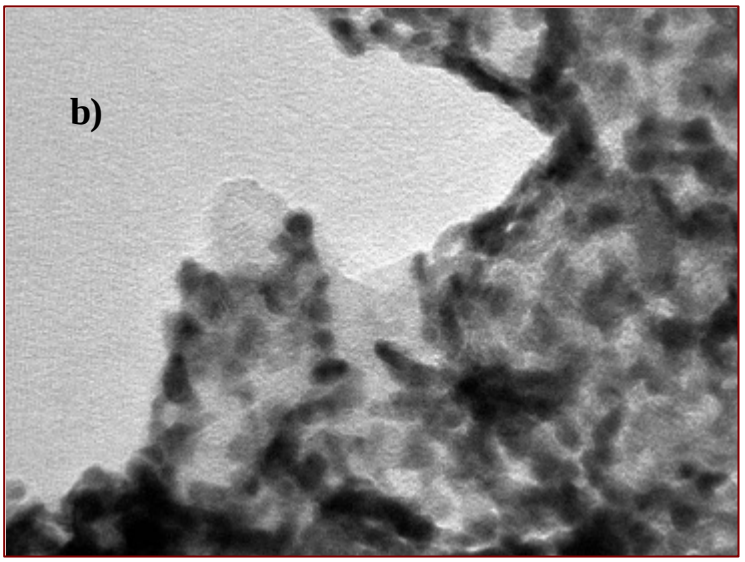

Fig II-2. Transmission electron micrographs of (a) 85% Pt-Ru/C and (b) 60% Pt/C catalysts.

II.2.2 ELECTROCHEMICAL CHARACTERIZATION

The influence of noble metal loading on the performance of the DMFC operating at low temperatures (30-60°C) was first investigated by steady-state polarization measurements, feeding 1 M MeOH solution to the anode and dry air to the cathode side under atmospheric conditions. Various test were carried out in order to optimize the Pt loading in each electrode for low temperature operation. Pt loadings ranging between 1 and 10 mg cm^{-2} were used for both anode and cathode. Figure II-3 shows the polarisation and power density curves obtained at 30°C for the different cells equipped with the various Pt loadings. In these experiments the same Pt loading was present at the anode and cathode. At 30°C the enhancement of power density, increasing the Pt loading from 3.5 to 5 $mg \cdot cm^{-2}$, is quite significant. Less significant is the improvement increasing the Pt loading from 5 to 10 $mg \cdot cm^{-2}$. Accordingly, 5 $mg \cdot cm^{-2}$ would be a suitable Pt loading for this application. This is confirmed by successive experiments at different temperatures.

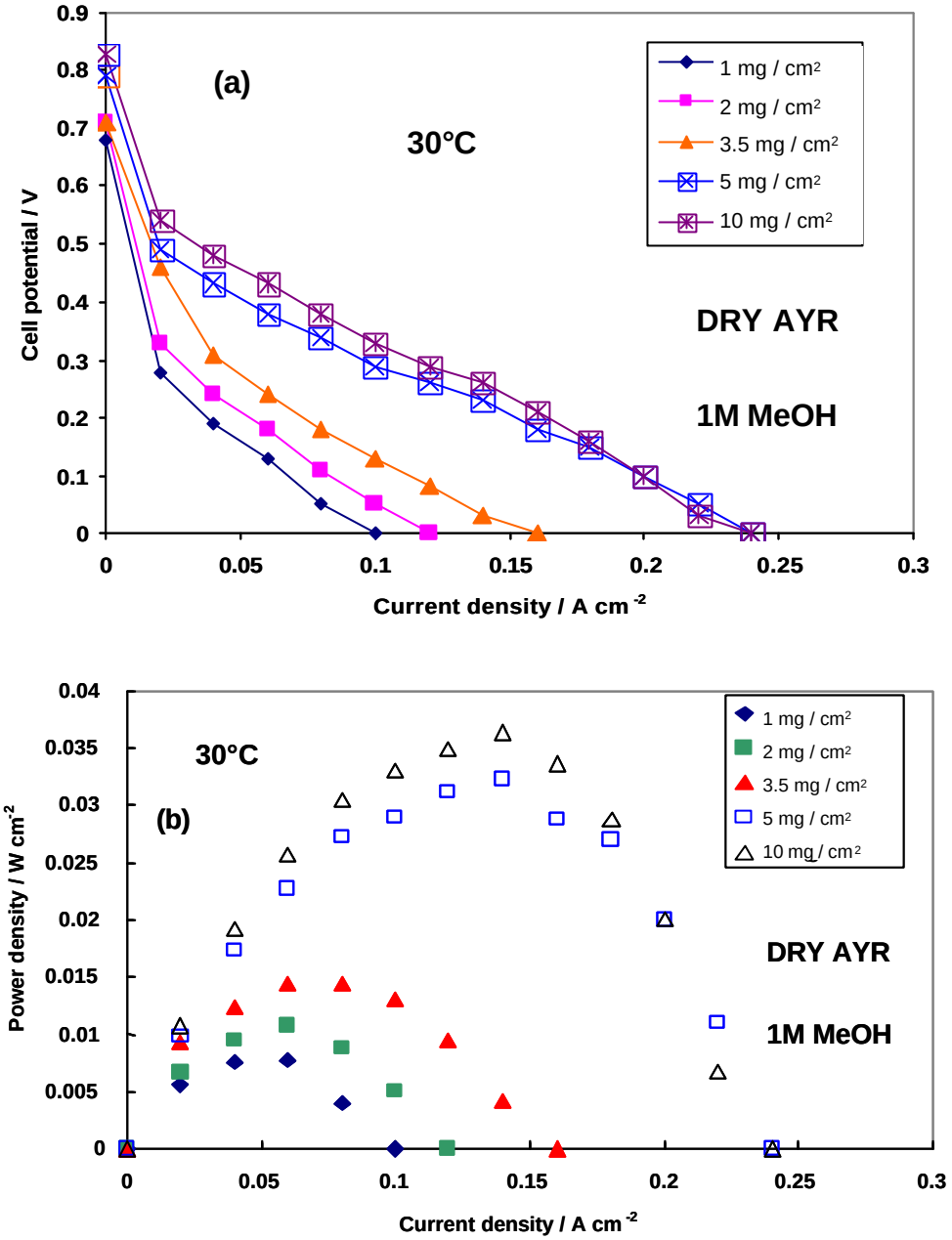

Fig. II-3 (a)-Polarization and (b)-power density curves at 30°C for the DMFC equipped with the 85%Pt-Ru (1:1)/C catalyst and the 60% Pt/C catalyst at various Pt loadings.

Figure II-4 shows the polarization and power density curves recorded at 60°C in the same conditions. The voltage losses decrease in the overall range of current densities as the Pt loading is increased from 1 to 5 mg·cm^{-2}; whereas, in the case of 10 mg·cm^{-2}, significant mass transfer limitations are observed at high currents. However, at 0.5 V, the current density for the cell equipped with 10 mg·cm^{-2} is higher than that recorded with 5 mg·cm^{-2} Pt content.

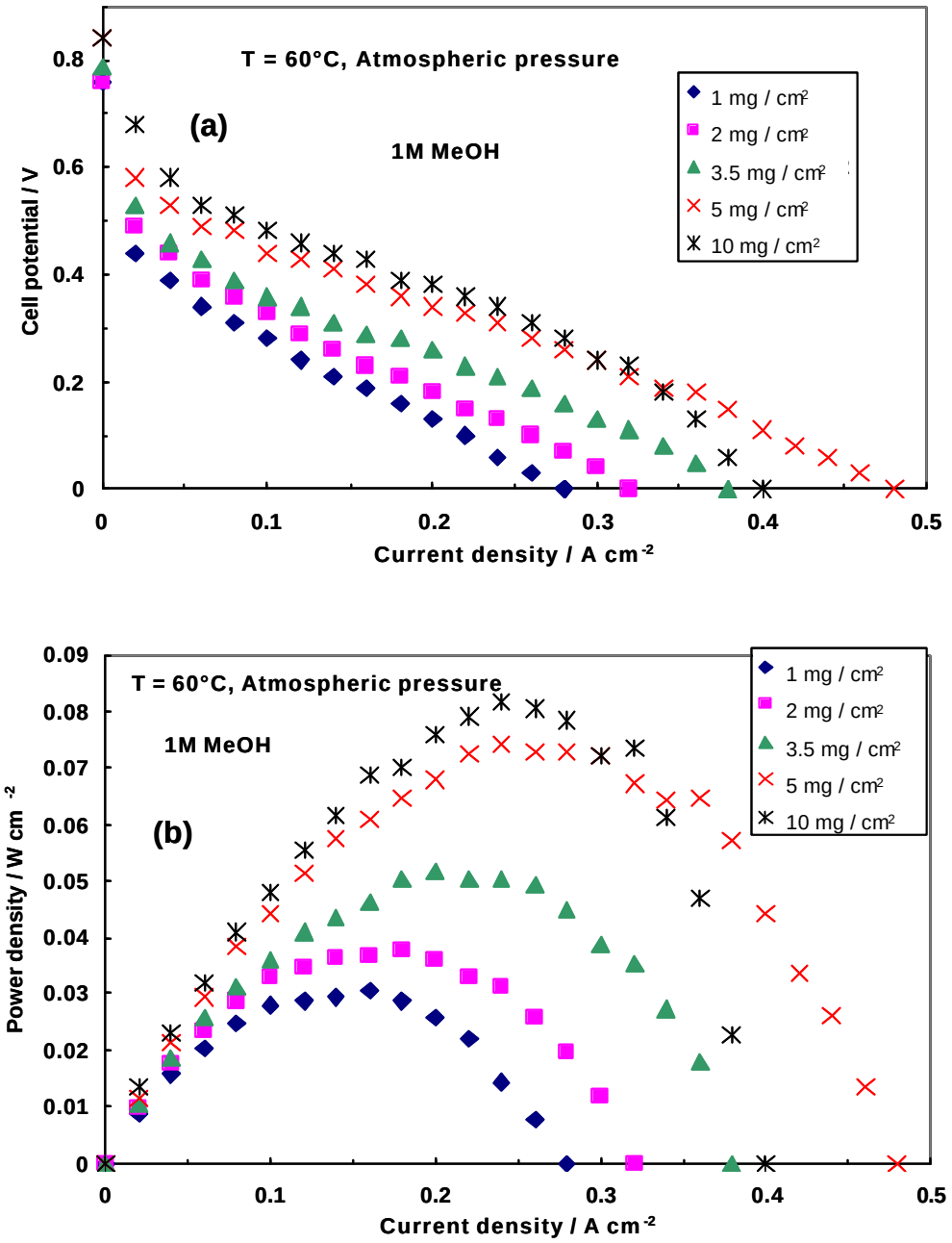

Fig. II-4 (a)-Polarization and (b)-power density curves at 60°C for the DMFC equipped with the 85% Pt-Ru (1:1) /C catalyst and the 60% Pt /C catalyst at various Pt loadings

A progressive increase of performance is recorded passing from 1 to 5 mg·cm^{-2}; the maximum power density increases from 30 to 75 mW·cm^{-2} at 60°C under atmospheric pressure. By further increasing the Pt loading at 10 mg·cm^{-2} only a slight increase of power density was recorded (81 mW·cm^{-2}). The performance is still better at very low current density in the activation region, but due to a decrease of the catalyst utilization (see below) the performance of the cell based on electrodes containing 10 mg Pt cm^{-2} is lower than

that expected. The performance is still better at very low current density in the activation region but a decrease of the catalyst utilization was observed in the latter case (10mg cm^{-2}). The reason is that the catalyst utilization decreases significantly when the Pt loading become excessive (Fig II-4). This can be explained by considering that the three phase reaction zone does not extend to the overall electrode thickness, but it is limited to the electrode – electrolyte interface. However, in the activation controlled region the performance for the 10 mg cm^{-2} Pt, loading cell is still better than the 5 mg cm^{-2} Pt cell since the decrease of the Pt utilization is less than 50%. At high current density, mass transfer limitations are observed in the case of the 10 mg cm^{-2} Pt cell. The mass transfer constraints are probably due to the large electrode thickness. These effects are also probably reflected in the stripping voltammogram of the anodic catalyst (Fig. II-5). This experiment was carried out *in situ* after methanol adsorption at 0.1 V for 30 min and successive washing with deaerated water for 15 min. *In situ* stripping voltammetry analysis of the anode catalyst (Fig. II-5) shows that the stripping charges associated with the adsorbed methanolic residues increase as a function of the Pt loading, but the electrochemical active surface area decreases as the Pt content is increased to 10 mg·cm^{-2}.

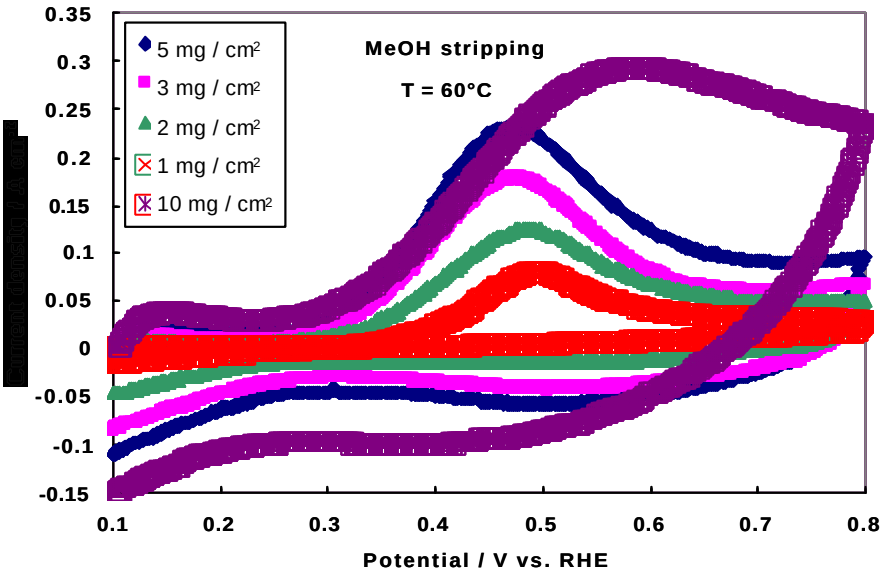

Fig. II-5 Methanolic residue stripping analysis in presence of various Pt loadings for the DMFC equipped with the 85% Pt-Ru (1:1) /C catalyst

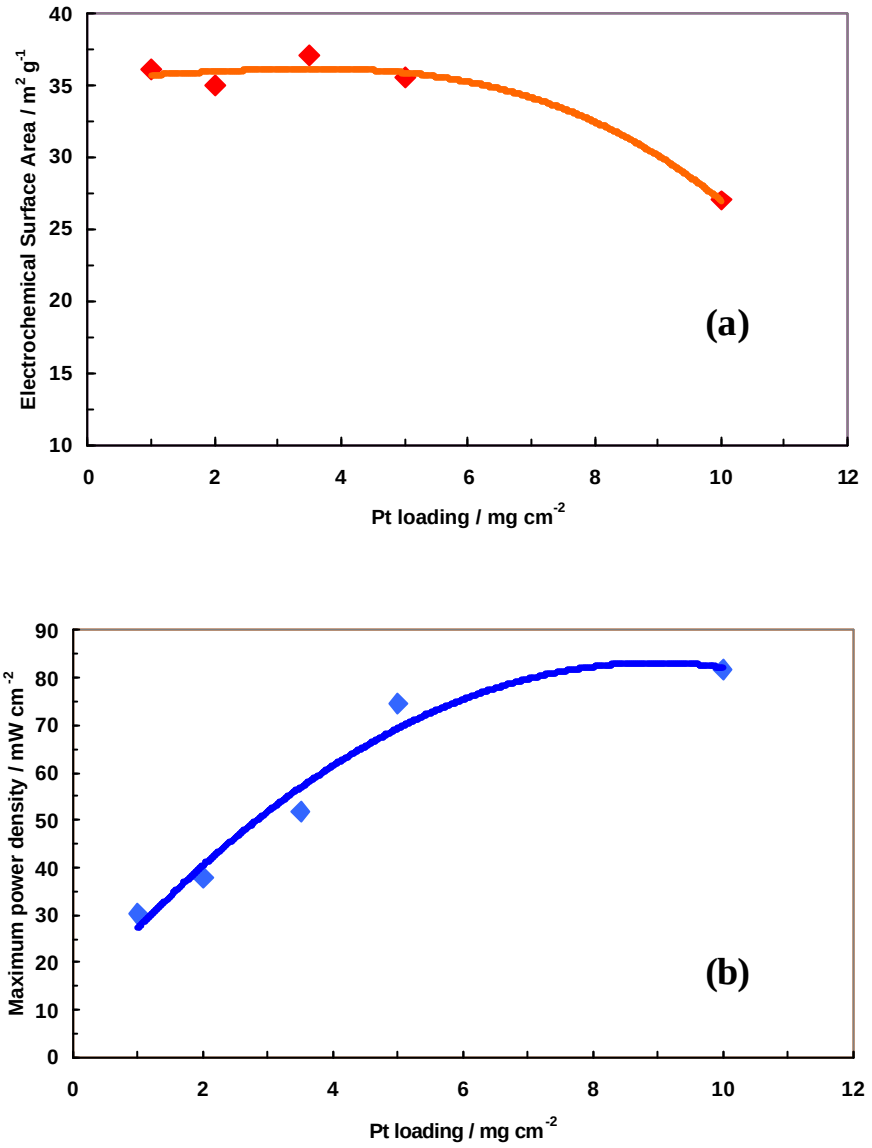

Fig. II-6 Effect of the Pt loading on the surface area (a) and maximum power density (b) of the DMFC equipped with the 85% Pt-Ru (1:1)/C catalyst and the 60% Pt /C catalyst at 60°C in dry air.

In Fig. II-6 the maximum power density and the electrochemical surface area are plotted as a function of Pt loading. It is also evident, from this analysis, that the performance of the DMFC does not improve significantly increasing the Pt loading from 5 to 10 mg·cm^{-2} on both electrodes at 60 °C (Figure 6a). Correspondingly, the catalyst utilization decreases significantly when the Pt loading is increased from 5 to 10 mg·cm^{-2} (Figure 6b). Methanol adsorption at 0.1 V occurs especially close to the electrode-electrolyte interface. However, in the activation controlled region the performance for the 10 mg·cm^{-2} Pt loading cell is still better than the 5 mg·cm^{-2} Pt-based cell, since the decrease of the Pt utilization is less than 50%. At high current density, mass transfer limitations are

also observed in the case of the 10 mg·cm^{-2} Pt cell, as above discussed. The mass transfer constraints are probably due to the large electrode thickness. These effects are also probably reflected in the stripping voltammogram of the anode (Fig. II-5). Accordingly, 5 mg·cm^{-2} Pt loading seems to be the optimal content in terms of maximum power density for low temperature (30-60°C) DMFCs. Similar behaviour is observed for the power density at 0.5 V as a function of Pt loading (Fig. II-7).

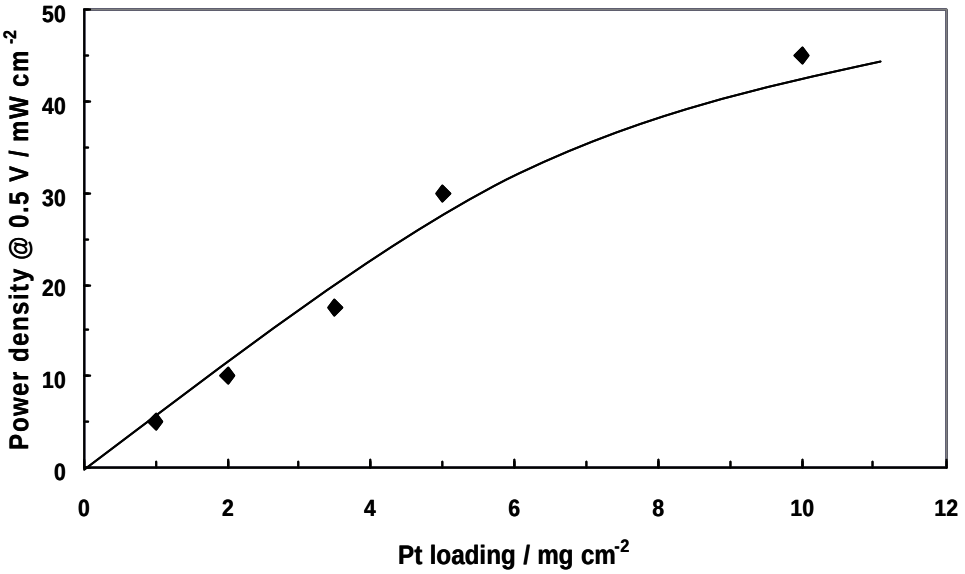

Fig. II-7. Variation of power density at 0.5 V as a function of Pt loading in DMFCs equipped with 85% Pt-Ru/C and 60% Pt/C catalysts. Cell temperature: 60°C.

Figure II-8 shows the influence of temperature on the single cell polarisation and power density behaviour for the cell equipped with 5 mg·cm^{-2} Pt loading on both anode and cathode compartments under ambient pressure. The power density increases from 32 to 75 mW·cm^{-2} passing from 30°C to 60°C, indicating the strong activation nature of the methanol electro-oxidation reaction.

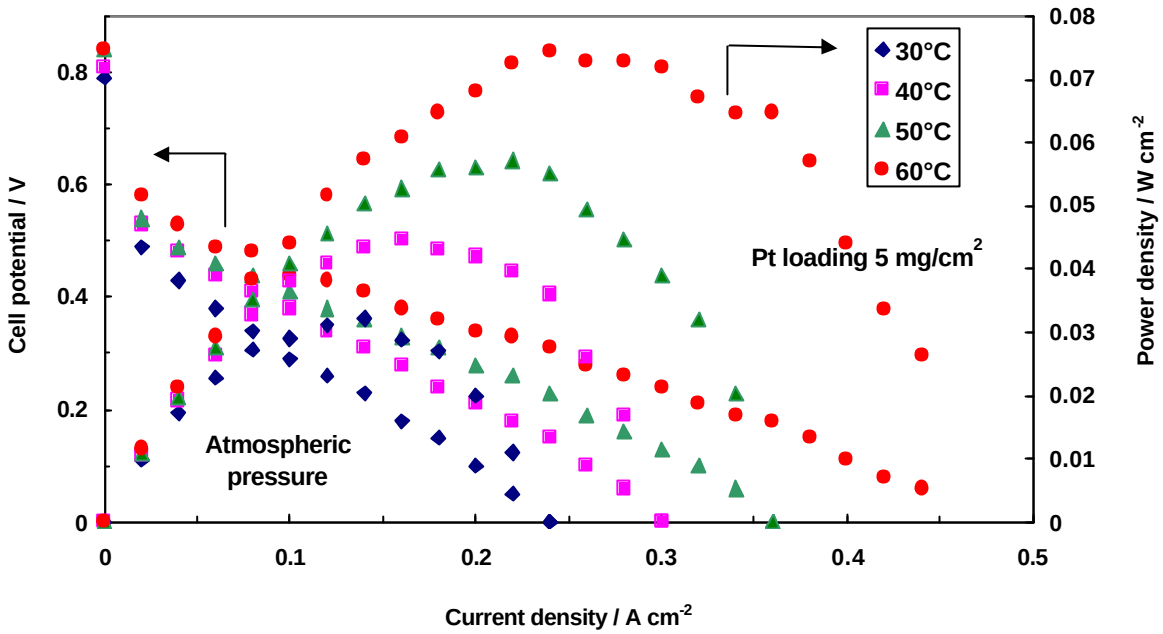

Fig II-8. Polarization and power density curves at various temperatures for DMFCs equipped with 85% Pt-Ru/C and 60% Pt/C catalysts with 5 mg cm^{-2} Pt loading under atmospheric pressure.

These findings are confirmed by the adsorbed methanolic residues stripping analysis carried out at various temperatures (Fig. II-9). Integrated charge and stripping potential provide information on the number and strength of the adsorbed species which participate to the rate determining step for methanol oxidation. The onset potential for the stripping of methanolic residues increases from 0.3 to 0.4 V as the temperature decreases from 60°C to 30°C (Figure 9). It appears that at 30°C the methanol adsorption does not reach a complete coverage at 0.1 V, whereas the coverage increases with temperature as reflected by the decrease of the hydrogen desorption peaks at low potentials. The stripping peak appears more sharp and increases in intensity as well as it shifts to lower potentials at higher temperatures reflecting faster desorption kinetics. Assuming that the methanolic residues are CO-like species and that the coverage at 60 °C is approaching the monolayer ($\theta = 1$), the electrochemical active surface area of the anode catalyst is about 36 m^2/g when the Pt loading is 5 $mg \cdot cm^{-2}$.

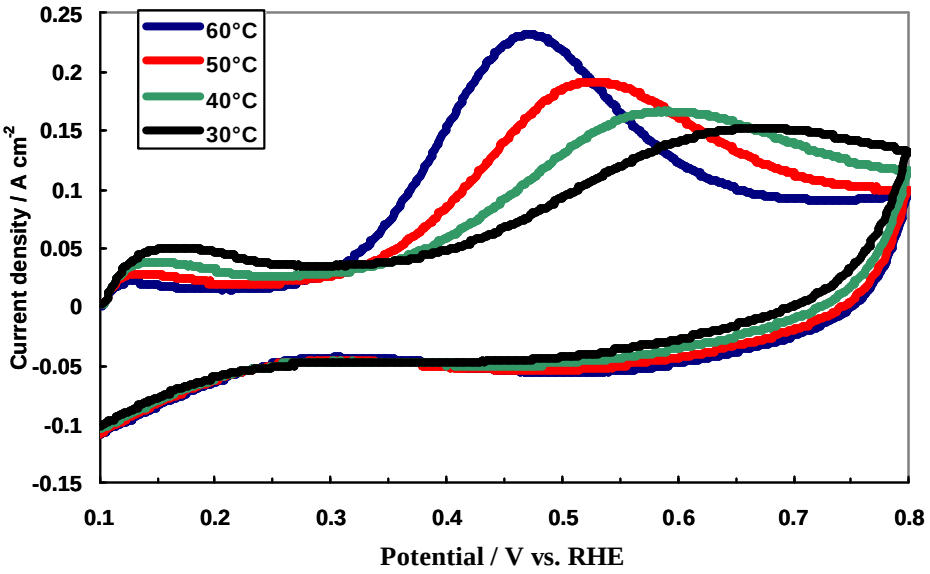

Fig II-9. *In situ* adsorbed methanolic residues stripping voltammetry at 85% Pt-Ru/C Nafion 117 membrane interface in the presence of 5 mg cm^{-2} Pt loading at different temperatures under the DMFC configuration

By increasing the cathode (air) pressure at 3 atm abs., the performance of the DMFC based on 5 mg·cm^{-2} Pt loading further increased reaching 90 mW·cm^{-2} (Fig. II-10).

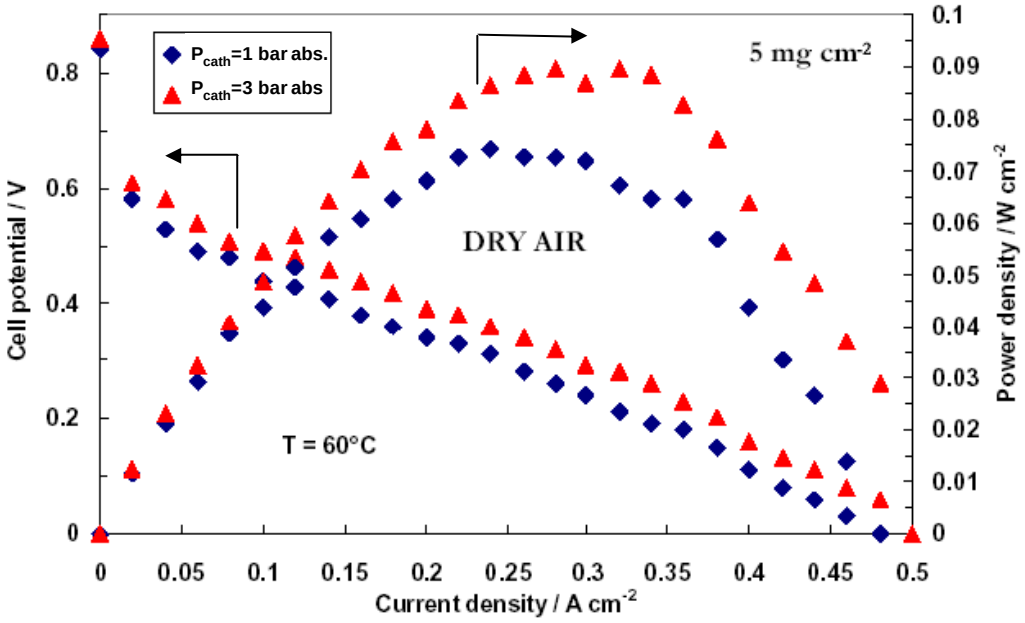

Fig. II-10. Polarization and power density curves at various pressures for DMFCs equipped with 85% Pt-Ru/C and 60% Pt/C catalysts with 5 mg cm^{-2} Pt loading

It is due to the beneficial influence of the increased oxygen partial pressure both on the kinetics of the cathode process and on counteracting the poisoning effect of the methanol crossing the membrane. A physical barrier to the methanol cross-over appears to be produced by the higher pressure at the cathode compartment, as confirmed by the methanol cross-over values recorded in the different pressure conditions at 60°C ($3.2*10^{-6}$ mol·min^{-1}·cm^{-2} under atmospheric pressure vs. $2.5*10^{-6}$ mol·min^{-1}·cm^{-2} with 3 atm abs. at the cathode side).

Figure II-11 shows that a decrease of the Pt loading in the anode from 5 to 2 mg·cm^{-2} does not significantly decrease the performance in the activation region. The maximum power density decreases by only 10%. Whereas, a decrease of Pt loading on both anode and cathode reduces significantly the performance both in the activation region and in terms of maximum power density. It is observed that the current density in the activation controlled region is mainly governed by the Pt loading at the cathode (Figure 11). This effect is clearly related to the methanol crossover which produces the poisoning of a significant portion of cathode catalyst surface.

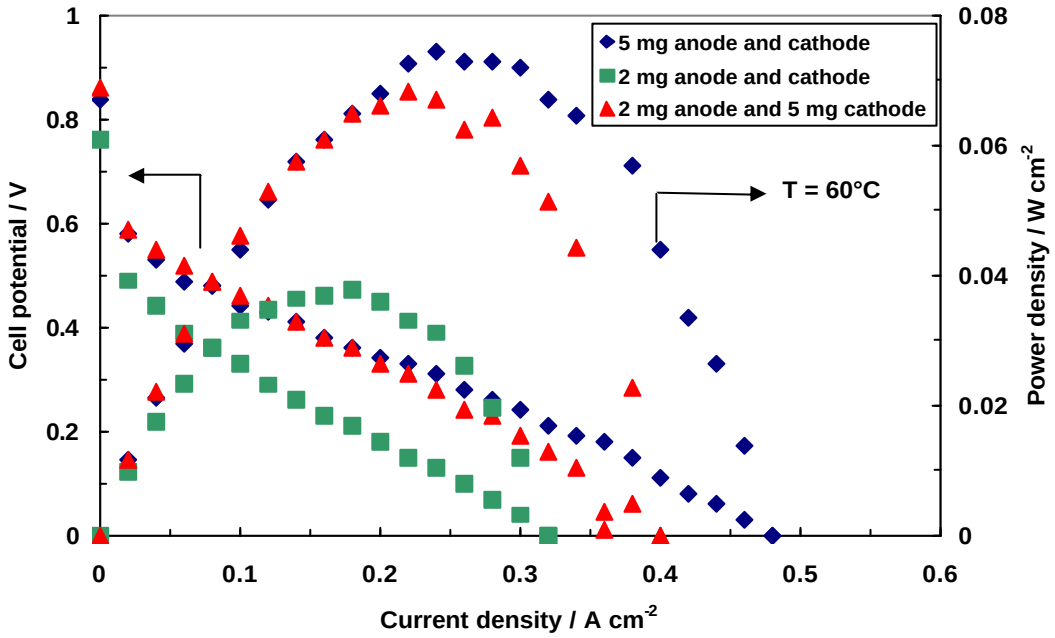

Fig. II-11. Influence of the different Pt loading at the anode and cathode side on the polarization and power density curves at 60°C for DMFCs equipped with 85% Pt-Ru/C and 60% Pt/C catalysts under atmospheric pressure

II.3 CONCLUSIONS

The influence of noble metal loading and catalyst utilisation on the electrochemical behaviour of low temperature (30°C-60°C) DMFCs was investigated by steady-state polarisations and adsorbed methanolic residues stripping voltammetry. From these analyses, 5 $mg \cdot cm^{-2}$ seems to be the most suitable Pt loading at the cathode for low temperature DMFC application. Whereas, 2 $mg \cdot cm^{-2}$ Pt loading at the anode is sufficient to achieve suitable performance. The maximum power density increased from 30 to 75 $mW\ cm^{-2}$ at 60°C passing from 1 to 5 $mg \cdot cm^{-2}$ Pt loading on both anode and cathode at ambient pressure, whereas only a slight increase was observed with 10 $mg \cdot cm^{-2}$, due to the decrease of catalyst utilization.

II.4 REFERENCES

[1] X. Ren, M.S. Wilson, S. Gottesfeld, *J. Electrochem. Soc.* 143, L12 (1996).

[2] L. Liu, C. Pu, R. Viswanathan, Q. Fan, R. Liu, E.S. Smotkin, *Electrochim. Acta* 43, 3657 (1998).

[3] A.S. Aricò, A.K. Shukla, K.M. el-Khatib, P. Cretì, V. Antonucci, *J. Appl. Electrochem.* 29, 671 (1999).

[4] H.G. Petrow, R.J. Allen, US Patent 3,992,331 (1976).

[5] A.S. Aricò, V. Baglio, A. Di Blasi, E. Modica, P.L. Antonucci, V. Antonucci, *J. Electroanal. Chem.* 557, 167 (2003).

CHAPTER III

INVESTIGATION OF PT-M/C AS DMFC CATHODE CATALYSTS

III. INTRODUCTION

The target of DMFC devices for portable applications is to work at relatively low temperatures and atmospheric pressure with high efficiency and performance. The effective operation at this low temperature is particularly challenging and requires innovation in different aspects of materials and system development. In particular, to address the poor reaction kinetics at the anode, high surface area catalysts composed of nanosized noble metal particles need to be developed and investigated for operation at low temperatures starting from sub-ambient to 60 °C [1-5]. Although, one of the main drawback of DMFC systems, i.e. the methanol cross-over through the membrane, is strongly depressed by the decrease of the operating temperature, this constraint affects the cathode performance even at low temperature by causing a mixed potential and poisoning of the cathode surface [5-10]. Accordingly, it is strongly necessary to develop methanol tolerant cathode catalysts with suitable activity at low temperature. Also in this case, a proper catalytic activity for achieving portable fuel cells performance targets is assured by noble metal catalysts properly modified with transition metals capable of reducing the adsorption of alcohols on the cathode surface [11-18].

Methanol crossover results in a significant loss in efficiency of a DMFC because two reactions compete on the Pt cathode i.e. O_2 reduction (ORR) and CH_3OH oxidation. One approach to solve this problem is to use an oxygen reduction catalyst, inactive towards methanol oxidation or having a high methanol tolerance [19].

Figure III-1 shows the electrochemical behaviour of the DMFC single cell together with the anode and cathode polarization curves. It appears that the DMFC performance is mainly limited by three effects: a mixed potential at the cathode that reduces the OCV, a strong activation control for the methanol eletro-oxidation process and a mass transport control affecting significantly both anode and cathode polarizations even at moderate current densities. These latter effects are possibly associated to the CO_2 removal at the anode and the flooding of the cathode by the water transported through the membrane.

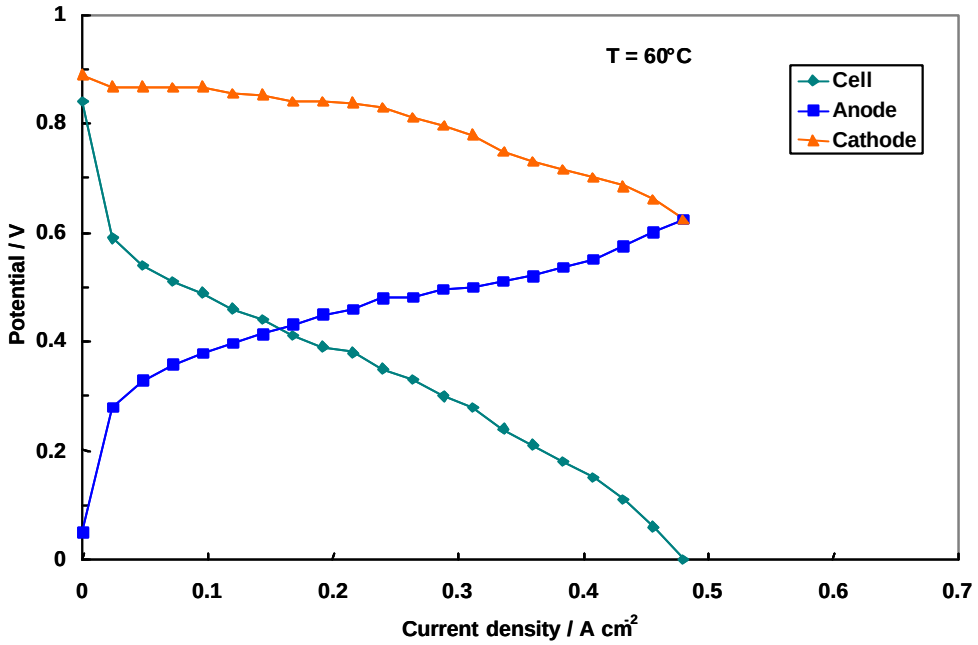

Fig. III-1. Anode, cathode and cell polarizations at 60°C for the DMFC based on PtRu/C and PtFe/C catalysts with 25% Nafion loading in the electrodes.

Thus, it is necessary to develop novel Pt based electrocatalysts that can catalyze the oxygen reduction but limit methanol oxidation. Many investigations have shown that some binary Pt based alloy catalysts, such as Pt–M, (where M = Co, Fe, etc.), exhibit an enhanced electrocatalytic activity for the ORR in comparison with Pt alone [20-25]. Such an activity enhancement was explained by the increased Pt d-band vacancy (electronic factor) and by the favorable Pt–Pt interatomic distance (geometric effect).

A relationship between the electrocatalytic activity and the adsorbate bond length has been predicted. Thus, a lattice contraction due to alloying would result in a more favorable Pt-Pt distance for the dissociative adsorption of O_2. Besides, the influence of electronic and geometric factors (Pt d-band vacancy and Pt- coordination numbers) and their relative effect on the H^+ chemisorption from the electrolyte occurs [26].

Watanabe et al. reported that, after electrochemical testing of a Pt-Fe alloy, the catalyst was covered by a thin Pt skin of less than 1 nm thick [27]. Moreover, they suggested that during the adsorption step, a π orbital of O_2 interacts with empty d orbitals of Pt and consequent back donation from the partially filled orbital of Pt to π^* (anti-bonding) molecular orbital of O_2. The increase in d band vacancies on Pt by alloying produces a strong metal–O_2 interaction. Such interaction weakens the O-O bonds resulting in bond cleavage and bond formation between O and H^+ of the electrolyte, thus improving the

ORR. One concern with Pt alloys in fuel cells is dissolution of transition metal. Pourbaix diagrams [28] indicate that most metals such as Co, Cu, Fe, Ni, etc. are soluble at a potential between 0.3 and 1 V versus SHE and at low pH values. The dissolution of the transition metal would cause an increase in surface area of the residual Pt catalyst.

There are different procedures related to catalyst preparation for DMFCs [29,30]. Preparation methods such as impregnation, colloidal deposition and surface reduction involve the adsorption of active compounds on a carbon black surface [31]. The synthesis of a highly dispersed electrocatalyst phase in conjunction with high metal loading on a carbon support is one of the present goals in DMFCs. One of the main requirements for an optimal electrocatalyst is its high dispersion. The mass activity (A/g Pt) of the catalyst for oxygen reduction is directly related to the degree of dispersion, since the reaction rate is generally proportional to its active surface area. Most of the previous studies were dealing with catalysts characterized by particle size larger than about 4 nm and low concentration of active phase on carbon due to the need of high temperature treatment to form bimetallic alloys of transition metals with Pt [1-5]. However, in order to accelerate the oxygen reduction process a suitable number of surface sites is necessary. Furthermore, various studies have indicated that for supported Pt/C catalysts a maximum catalytic activity occurs at about 3 nm as a suitable compromise between number of sites and crystallographic phases with low Miller index characterized by high intrinsic activity [32].

III.1 EXPERIMENTAL

A 60 wt% Pt/Vulcan XC-72R was prepared starting from chloroplatinic acid by using the sulfite-complex route [33]. A 60 wt% Pt-Fe/Vulcan XC-72R, a 60 wt% Pt-Co/Vulcan XC-72R and a 60 wt% Pt-Cu/Vulcan XC-72R with a catalyst atomic composition Pt_3M_1 were prepared starting from PtOx/Vulcan XC-72R by employing an incipient wetness method [34]. The bimetallic catalysts were reduced in a H_2 stream at room temperature. The obtained catalysts were characterized by recording the powders X-ray diffraction (XRD) pattern on a Philips X-pert 3710 X-ray diffractometer using Cu Kα radiation operating at 40 kV and 30 mA. The peak profile of the (220) reflection in the face centered cubic structure was obtained by using the Marquardt algorithm and used to calculate the crystallite size by using the Debay-Sherrer equation. X-ray Fluorescence analysis of the catalysts was carried out by a Bruker AXS S4 Explorer spectrometer operating at a power

of 1 kW and equipped with a Rh X-ray source, a LiF 220 crystal analyzer and a 0.12° divergence collimator. The Pt/M atomic ratio was determined in all catalyst samples. Table III-1 shows the physico-chemical characteristics of the carbon supported Pt and Pt-M catalysts. To prepare the electrodes, a thin diffusion-layer comprising acetylene black and 20 wt% Teflon was firstly pasted onto a carbon cloth followed by the catalyst layer consisting of the catalyst with 15 wt% Nafion. An in-house 85% Pt-Ru alloy (1:1)/C catalyst was employed at the anode [5] whereas the 60% Pt/C and Pt-M/C catalysts were utilized for cathode fabrication. A Pt loading of 5 mg cm^{-2} was used for both anode and cathode. A Nafion 117 membrane was used as electrolyte. Membrane-electrode assemblies (MEAs) were formed by a hot-pressing procedure [35] and subsequently installed in a fuel cell test fixture of 5 cm^2 active area. For single cell polarization experiments, aqueous methanol (1M) was pre-heated at the same temperature of the cell and fed to the anode chamber of the DMFC through a peristaltic pump; dry air, pre-heated at the same temperature of the cell, was fed to the cathode. Atmospheric pressure in the anode and cathode compartments was used for all experiments. Reactant flow rates were 2 ml min^{-1} and 350 ml min^{-1} for methanol/water mixture and air stream, respectively. Single cell performances were investigated by steady-state galvanostatic polarization measurements. In half-cell polarization studies a three-electrode configuration was used. Hydrogen was fed to the cathode that was used as both counter and reference electrode. The anode polarization measurements were carried out by potentiodynamic sweeps at a scan rate of 5 mV s^{-1}. Data have not been corrected for the IR-drop. The cathode potential was deduced by adding the anode potential to the cell voltage.

In situ stripping voltammetry of adsorbed methanolic residues at the anode under normal operation (1 M CH_3OH feed with a flow of 2 ml min^{-1}) was carried out at 60°C under DMFC configuration following a procedure previously reported [5].

III. 2 RESULTS AND DISCUSSION

III.2.1 PHYSICO-CHEMICAL CHARACTERIZATION

XRD patterns of Pt/C and Pt-M/C catalysts are reported in Fig. III-2. They show the typical fcc crystallographic structure of Pt. A moderate degree of alloying was found for Pt-Fe catalysts whereas the degree of alloying was slightly larger for Pt-Co/C and

significantly larger for Pt-Cu/C compared to Pt-Fe by using the same procedure. This is indicated by the decrease of the lattice parameter (Table III-1).

Table III-1. Physicochemical characteristics of Pt and Pt-M/C catalysts

Catalysts	Crystallite / nm	A_0 / nm	Pt/M at. (XRF)
60%Pt/C	**2.8**	**0.392**	**-**
60%Pt-Fe/C	**2.4**	**0.390**	**3.33**
60%Pt-Cu/C	**2.1**	**0.387**	**3.79**
60%Pt-Co/C	**2.3**	**0.389**	**3.50**

Taking into account that chemisorption of oxygen on the electrocatalysts is the first step of the ORR, the geometrical influence of the Pt lattice constant is quite significant for the overall reaction [36]. A contraction of Pt lattice constant facilitates the dissociative O_2 adsorption, thus the catalyst more strongly binds atomic oxygen [36]. As previously shown in the literatures, Pt-Fe catalysts with small lattice constant contraction show a significant enhancement of the electrocatalytic activity for ORR [12]. The lattice constant contraction obtained by using this low temperature preparation route is small compared to Pt-Fe catalyst obtained by carbothermal reduction at high temperatures [13]. Although a large contraction in Pt-Fe lattice is favourable in terms of specific activity, recent studies have shown that catalyst treatment at intermediate reduction temperatures, resulting in small Pt-Fe lattice contraction, are associated with a mass activity significantly higher than bare Pt catalysts [13].

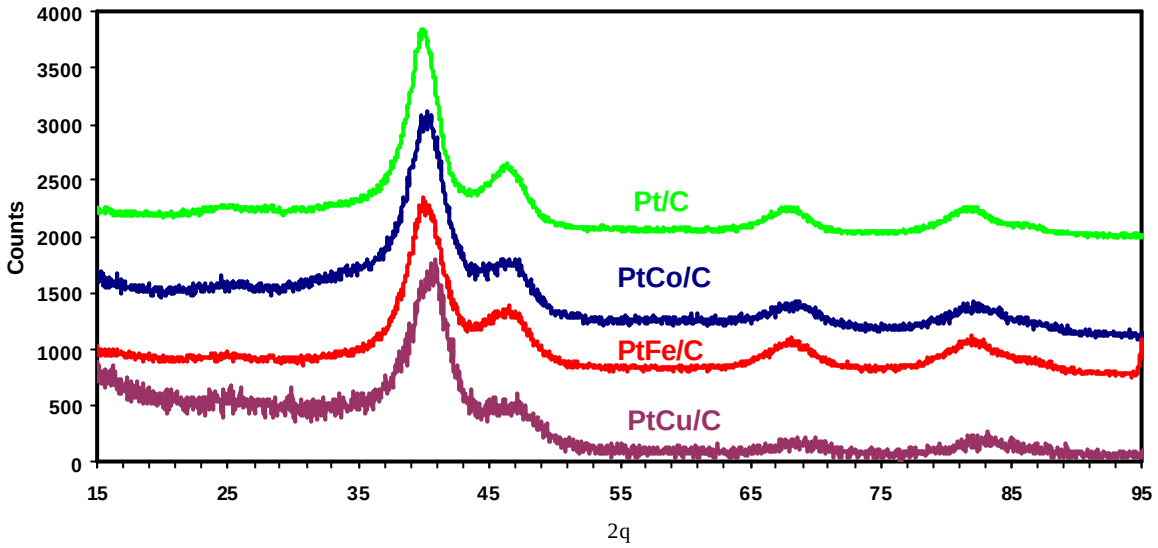

Fig. III-2. XRD patterns of Pt and Pt-based bimetallic catalysts.

TEM analysis of the catalysts shows a crystallite size for the catalysts comparable to that found by XRD measurements and a homogeneous distribution of fine metal particles on the support, despite of the high metal concentration on carbon (Fig. III-3).

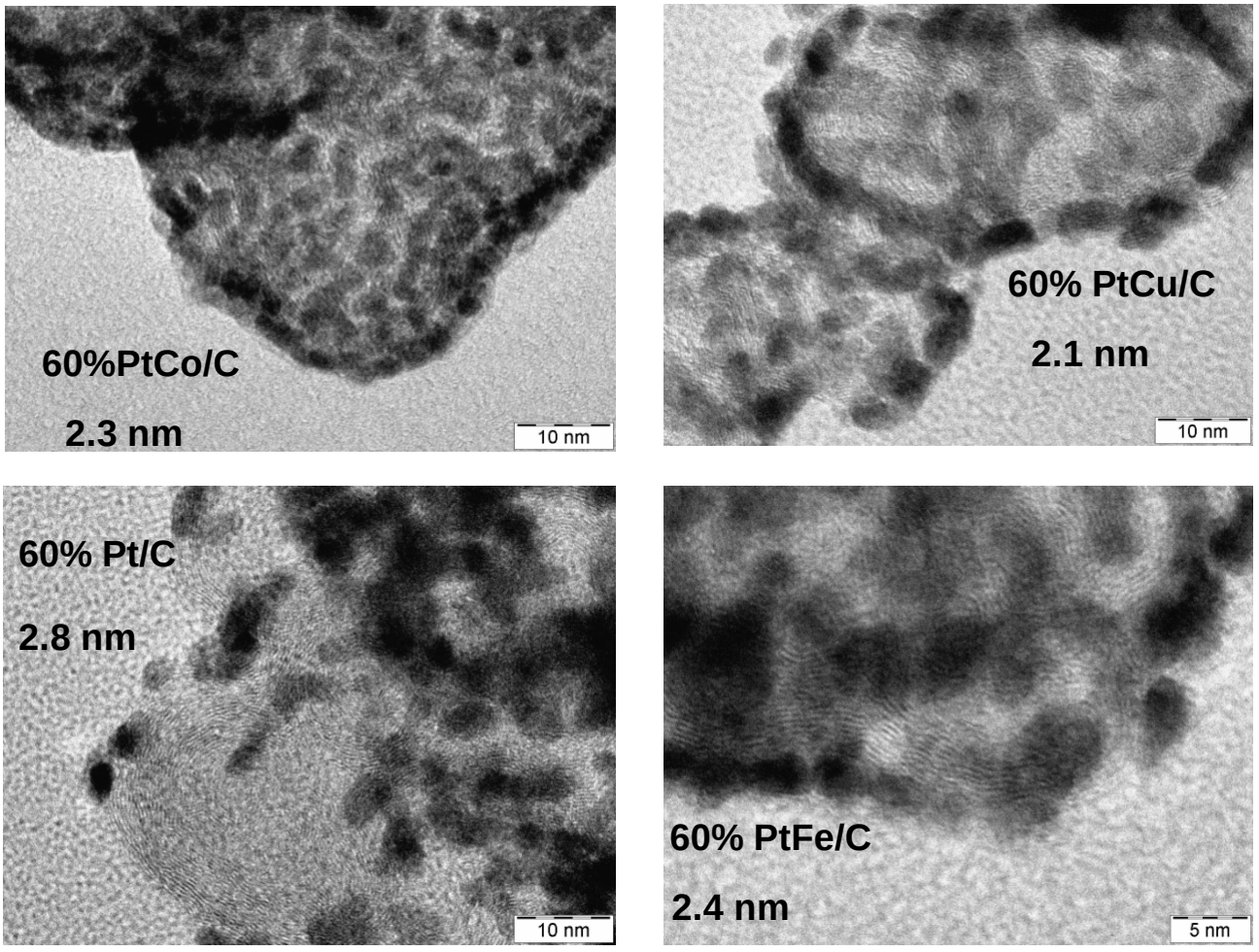

Fig. III-3. TEM micrographs of Pt and Pt-based bimetallic catalysts.

III.2.2 ELECTROCHEMICAL CHARACTERIZATION

The cathode catalysts were electrochemically investigated in a DMFC, by using a Pt-Ru/C catalyst as anode. The Pt loading was 5 mg cm^{-2} for both electrodes.

The Pt-Fe/C (2.4 nm) performed better than the Pt/C, Pt-Cu/C and Pt-Co/C catalysts with similar particle size (2.1-2.8 nm) at 60 °C (Fig. III-4). In fact, the maximum power density recorded with Pt-Fe/C as cathode catalyst at 60°C was about 75 mW cm^{-2}. At 0.5 V the current density was about 80 mA cm^{-2}. The cell equipped with the Pt-Cu/C catalyst at the cathode showed a lower performance in all the range of temperatures. A maximum power density of 58 mW cm^{-2} was recorded at 60°C under atmospheric pressure. At 0.5 V the current density was about 60 mA cm^{-2} at 60°C. The cell based on Pt-Co/C catalyst showed a maximum power density similar to that observed for the PtCu-based cell (about 60 mW cm^{-2}), whereas at 0.5 V the current density was about 70mA cm^{-2} at 60°C. Lower performances (55 mW cm^{-2} maximum power density; current density at 0.5 V close to 55 mA cm^{-2}) were recorded with the cell equipped with the bare Pt/C cathode catalyst.

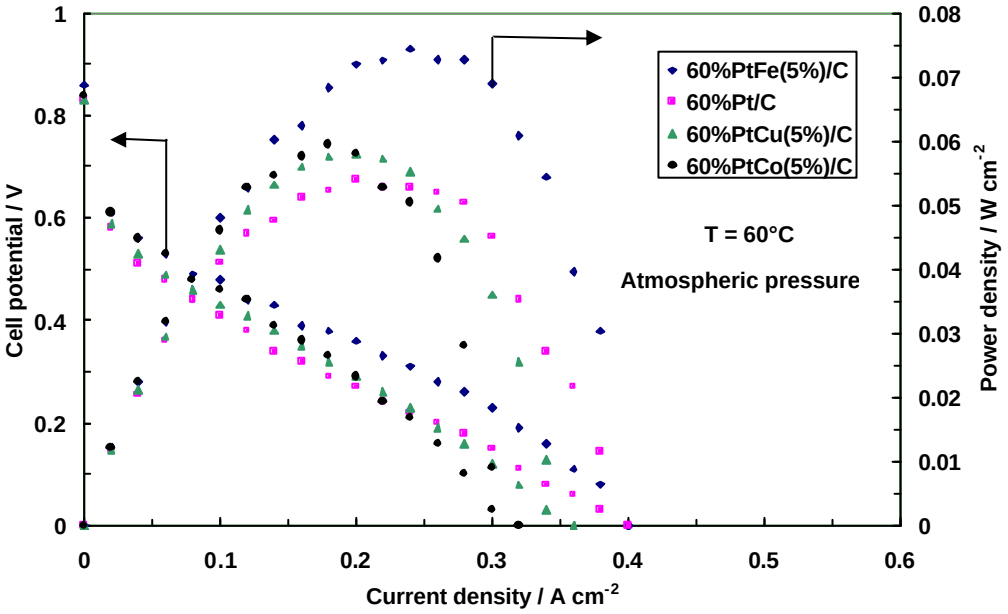

Fig. III-4. Polarization and power density curves for the DMFCs equipped with the various cathode catalysts at 60°C under atmospheric pressure

The better performance of Pt-Fe catalyst for ORR is also confirmed by the cathode polarization curves (Fig. III-5) that show almost the same trend of the cell polarizations, since the same anode was used in all the experiments.

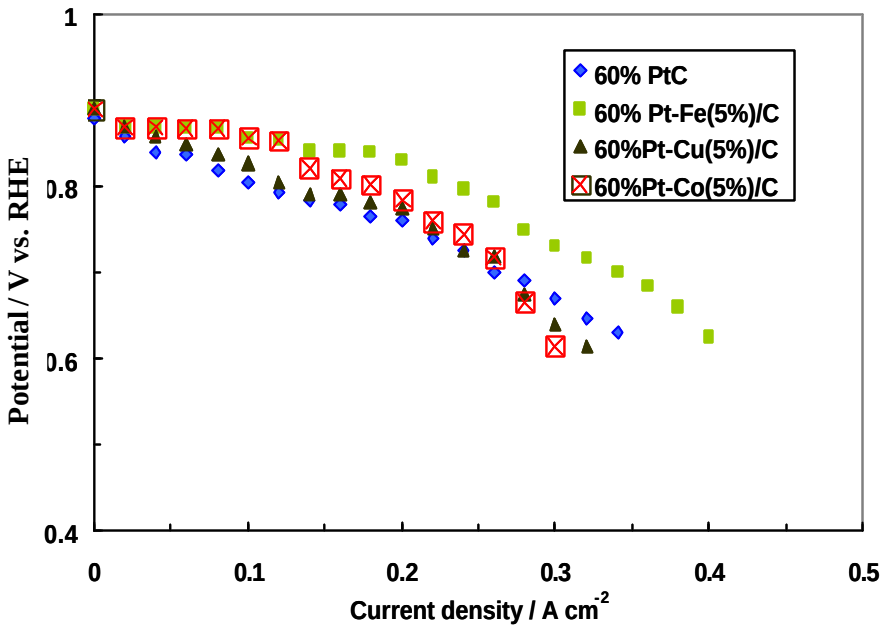

Fig. III-5. Cathodic polarization curves for DMFCs based on the different cathode catalysts recorded at 60°C under atmospheric pressure

At low current densities, also the Pt-Co/C catalyst shows a proper combination of methanol tolerance and oxygen reduction activity properties. Yet, these suitable characteristics are lost at high current densities. Methanolic residues stripping analysis (Fig. III-6) shows that this enhanced activity may derive from better methanol tolerance and higher intrinsic catalytic activity for oxygen reduction. The presence of a significant current density in the hydrogen desorption region (E<0.4 V vs. RHE) even after methanol adsorption, not observed for the other catalysts, indicates suitable methanol tolerance properties. The positive shift of the potential for PtO reduction is associated with a better intrinsic catalytic activity. The electrochemical active surface area as derived by the methanolic residues stripping analysis is larger for catalysts with smaller particle size (30.2 m^2/g for PtCu/C, 24.4 m^2/g for PtFe/C and 20.9 m^2/g for Pt/C). Yet, it appears that the small variation of electrochemically active surface area does not play the same role of the increase of methanol tolerance and intrinsic catalytic activity.

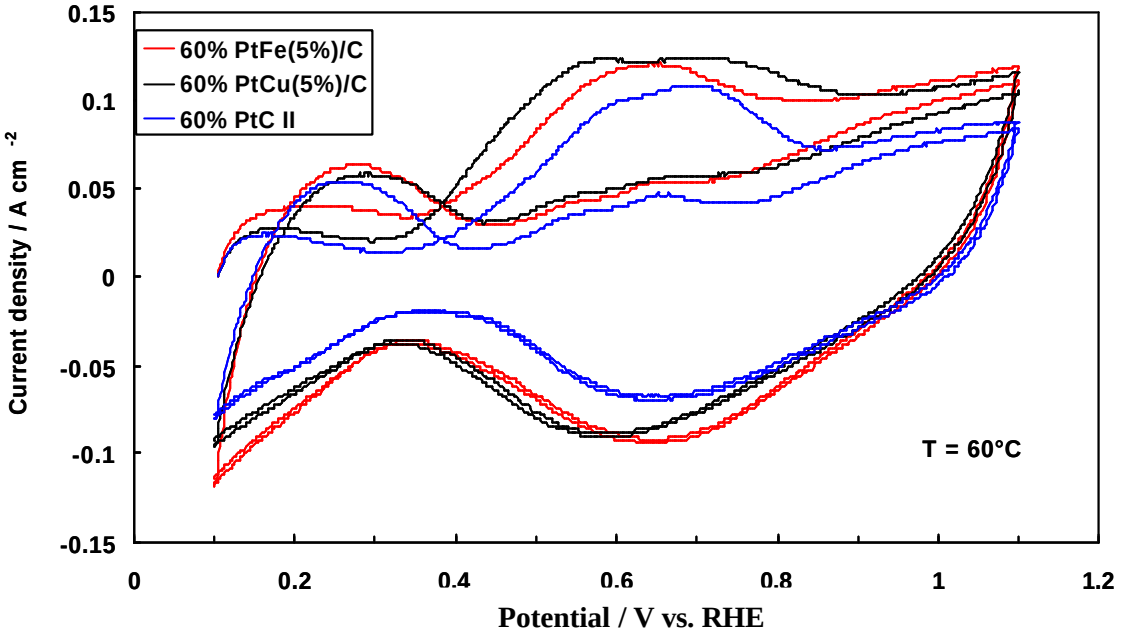

Fig. III-6. Adsorbed methanolic residues stripping voltammetry at a scan rate of 50 mV sec^{-1} for the different cathode catalysts at 60°C.

The enhanced catalytic activity for Pt-Fe catalysts has been attributed to the presence of a Pt skin over the alloy together with an electronic effect induced by Fe on Pt, as previously reported by Watanabe et al. [11]. The formation of the Pt skin probably occurs because iron on the surface leaches out of the alloy during operation in acidic electrolytes, while Pt atoms are redeposited and rearranged on the surface. For what concerns the electronic effect, it was emphasized that the electronic structures of the Pt skin layers are altered by the underlying alloy substrates, which in turn facilitates the electron transfer to oxygen molecules [11]. On the other hand, Li et al. claimed that the improvement in the performance of Pt–Fe/C for ORR may be partly due to the higher peroxide decomposition activity of Pt in presence of dissolved Fe favoring the 4 e transfer route [34]. In this respect, EDX measurements after operation showed a decrease in Fe content, revealing a partial ion dissolution during operation [36].

III.2.3 INFLUENCE OF IONOMER LOADING

The influence of the ionomer loading on the performance of the DMFC was investigated in order to increase the catalyst utilization, in particular when a high Pt loading is used (5 mg cm^{-2}). A comparison of the DMFC performance at 30°C for MEAs equipped with electrodes containing 15, 25 and 33% Nafion loading is presented in Fig. III-7. The OCV and the performance, both in terms of maximum power density and short circuit current density, were higher for the cells based on electrodes containing 25% Nafion.

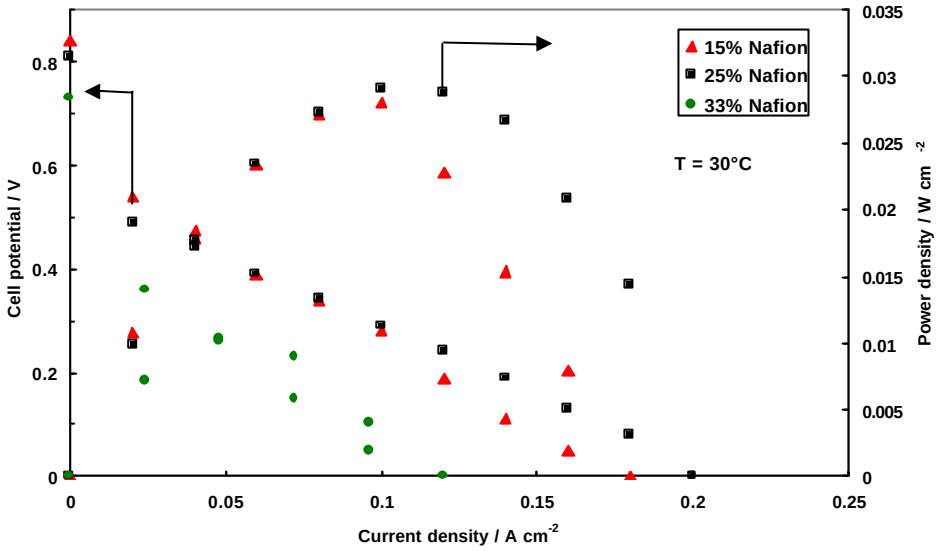

Fig. III-7. Polarization and power density curves at 30°C for the DMFCs equipped with the 85% Pt-Ru (1:1) /C catalyst and the 60% Pt-Fe(5%) /C catalyst, containing different Nafion loading on both electrodes. 5 mg Pt cm^{-2}. Dry air, atmospheric pressure.

By increasing the temperature up to 60°C, the performance increased due to the enhanced methanol oxidation and oxygen reduction kinetics (Fig. III-8). A maximum power density of 87 mW cm^{-2} was obtained for the cell equipped with 25% Nafion loading in the electrodes. For what concerns the maximum power density, the DMFC based on 25% Nafion loading electrodes was the most performing both at 30 and 60°C. This was probably due to a good compromise between the cell resistance and the extension of the three-phase reaction zone.

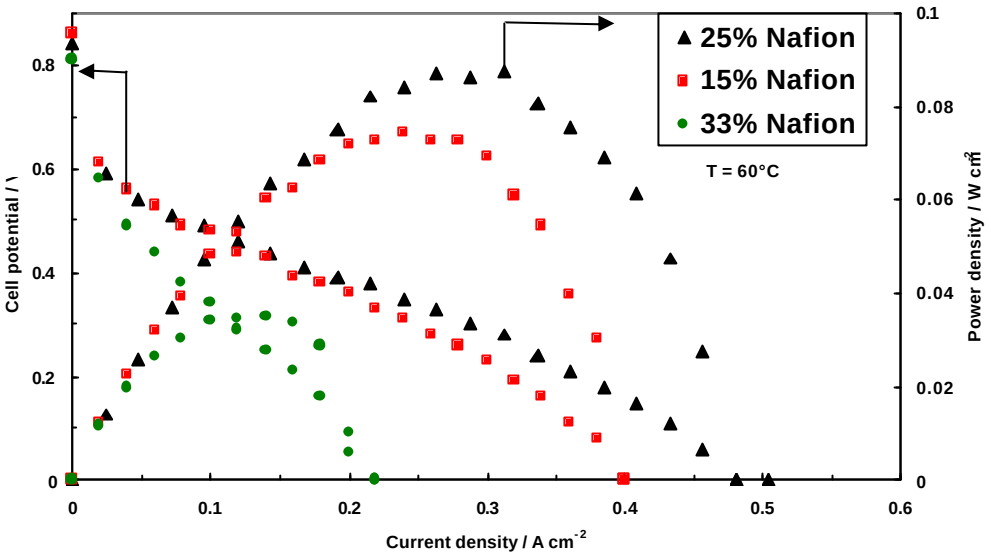

Fig. III-8. Polarization and power density curves at 60°C for the DMFCs equipped with the 85% Pt-Ru (1:1) /C catalyst and the 60% Pt-Fe(5%) /C catalyst, containing different Nafion loading on both electrodes. 5 mg Pt cm^{-2}. Dry air, atmospheric pressure.

Figure III-9 shows an increase of cell resistance as the Nafion loading in the electrodes is increased. This phenomenon is quite significant with 33% Nafion content at 30°C. It explains the poor performance recorded by the cell containing this amount of ionomer. Also the catalytic activity plays a significant role in determining the performance of the cell.

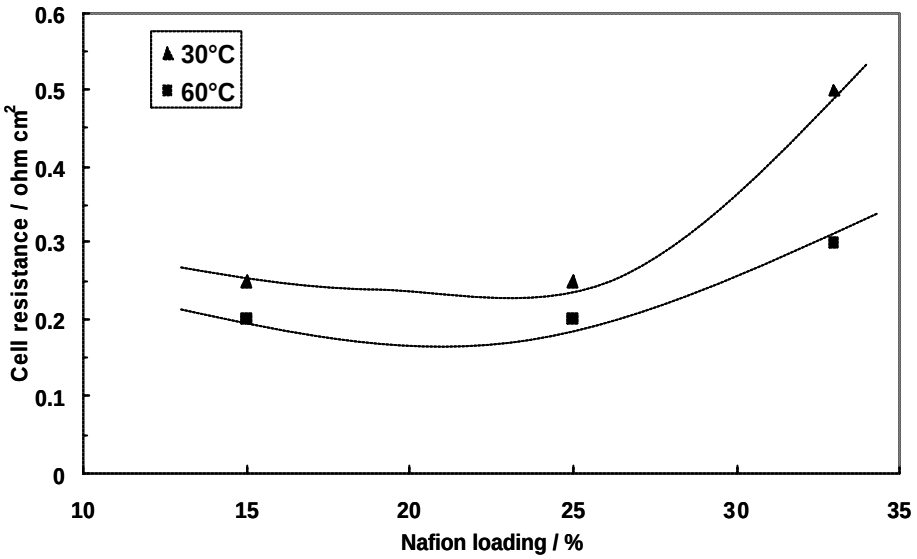

Fig. III-9. Variation of cell resistance as a function of Nafion loading in the electrodes

Accordingly, adsorbed methanolic residues stripping analyses were carried out on both anode and cathode of the cells characterized by different amounts of Nafion ionomer in the catalytic layer. Figure III-10 clearly shows a shift of the peak of MeOH residues stripping towards higher potential as the Nafion loading in the electrode is increased. An increase of the acidity level in the anodic layer as a consequence of the increased ionomer content from 15 wt% to 25 wt% causes a shift to higher potentials of the adsorbed methanolic residue stripping peak. It is well known that the kinetics of methanol electro-oxidation are enhanced in alkaline solutions with respect to acid electrolytes. Thus, the observed variation in the CV profile mainly reflects a change in the local pH. The addition of Nafion ionomer to the catalytic layer, should enhance the triple-phase boundary. Yet, an excessive ionomer content may also cause an increase of ohmic drop as it may be envisaged in the CV profile for the layer containing 33 wt% ionomer.

The onset stripping potential is the same for the 15 and 25% Nafion based electrodes, but the increase of active area for the 25% Nafion loading electrode produces a slight shift of the peak potential towards more positive values.

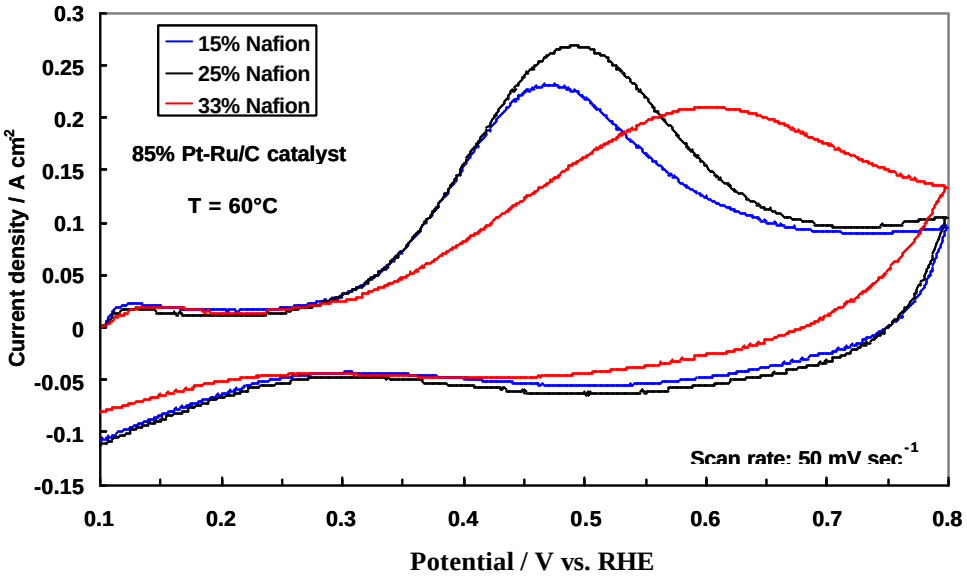

Fig. III-10. Methanolic residues stripping analysis at 60°C in the presence of different Nafion loading for the DMFCs equipped with the 85% Pt-Ru (1:1) /C catalyst.

Upon increasing the cathode pressure at 3 atm abs., the performance increased for all the MEAs equipped with the different Nafion loading (Fig. III-11), also due to the influence of the oxygen partial pressure in counteracting the poisoning effects by the cross-over of methanol. In these conditions, the maximum power density was obtained always with the 25% Nafion loading and approached 100 mW cm^{-2} (Fig. III-11).

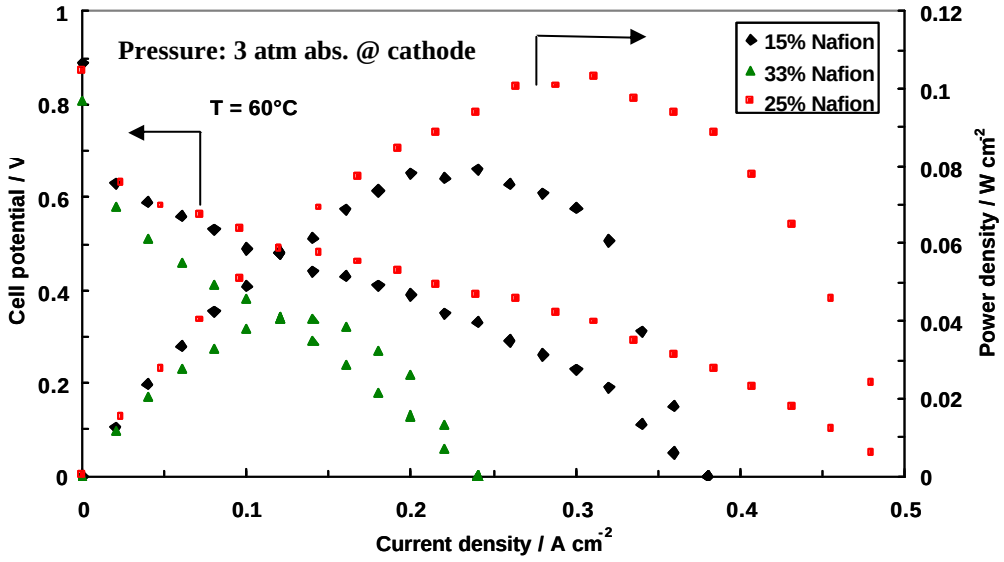

Fig. III-11. Polarization and power density curves at 60°C for the DMFCs equipped with the 85% Pt-Ru (1:1) /C catalyst and the 60% Pt-Fe(5%) /C catalyst, containing different Nafion loading on both electrodes. 5 mg Pt cm^{-2}. Dry air, 3 atm abs. pressure at the cathode.

III. 3. CONCLUSIONS

A preparation procedure was developed to modify the Pt catalysts with transition metals. A moderate degree of alloying was obtained with Pt-Fe/C cathode catalyst by using this low temperature preparation route. Whereas, the degree of alloying was slightly larger for Pt-Co/C and significantly larger for Pt-Cu/C compared to Pt-Fe by using the same procedure. High surface area carbon supported bimetallic Pt-Co, Pt-Cu and Pt-Fe catalysts were investigated for the oxygen electro-reduction process in low temperature direct methanol fuel cells (60 °C) and compared to Pt/C catalysts. Adsorbed methanolic residues stripping analysis showed a better methanol tolerance and an enhanced activity towards oxygen reduction in the case of the Pt-Fe system. An improvement of the DMFC single cell performance was also observed in the presence of Pt-Fe catalysts.

Moreover, the influence of the ionomer loading on the performance of the DMFC was investigated. A compromise in terms of conductivity within the layer and catalyst utilization was observed for a Nafion loading of 25 wt%. The highest power density recorded with electrodes containing 25% Nafion loading was approaching 90 mW cm^{-2} at 60 °C in the presence of air at atmospheric pressure.

III.4 REFERENCES.

[1] T.C. Deivaraj, J.Y. Lee, J. Power Sources 142 (2005) 43.

[2]K.-T. Jeng, C.-C. Chien, N.-Y. Hsu, S.-C. Yen, S.-D. Chiou, S.-H. Lin, W.-M. Huang, J. Power Sources 160 (2006) 97.

[3 Z.-G. Shao, F. Zhu, W.-F. Lin, P.A. Christensen, H. Zhang, B. Yi, J. Electrochem. Soc. 153 (2006) A1575.

[4] A.S. Aricò, V. Baglio, A. Di Blasi, E. Modica, P.L. Antonucci, V. Antonucci, J. Electroanal. Chem. 557 (2003) 167.

[5] A.S. Aricò, V. Baglio, A. Di Blasi, E. Modica, G. Monforte, V. Antonucci, J. Electroanal. Chem. 576 (2005) 161.

[6] L. Jorissen, V. Gogel, J. Kerres, J. Garche, J. Power Sources 105 (2002) 267.

[7] J.R. Salgado, E. Antolini, E. R. Gonzalez, Applied Catal.B: Envirom. 57 (2005) 283.

[8] U.A. Paulus, A. Wokaun, G.G. Scherer, T.J. Schmidt, V. Stamenkovic, V. Radmilovic, N.M. Markovic, P.N. Ross, J Phys. Chem. B 106 (2002) 4181.

[9] S. Mukerjee, S. Srinivasan, M.P. Soriaga, J.M. Mc Breen, J.Electrochem.Soc. 142 (1995) 1409.

[10] T.J. Schmidt, U.A. Paulus, H.A. Gasteiger, R.J. Behm, J. Electroanal. Chem. 508 (2001) 41.

[11] T. Toda, H. Igarashi, M. Uchida, M. Watanabe, J. Electrochem. Soc. 146 (1999) 3750.

[12] W. Li, W. Zhou, H. Li, Z. Zhou, B. Zhou, G. Sun, Q. Xin, Electrochim. Acta 49 (2004) 1045.

[13] M. Min, J. Cho, K. Cho, H. Kim, Electrochim. Acta 45 (2000) 4211.

[14] R.C. Koffi, C. Coutanceau, E. Garnier, J.-M. Leger, C. Lamy, Electrochim.Acta 50 (2005) 4117.

[15] H. Uchida, H. Ozuka and M. Watanabe, Electrochim. Acta 47 (2002) 3629.

[16] A.K. Shukla and R.K. Raman, Annual Review of Materials Research 33 (2004) 155.

[17] A.K. Shukla, R.K. Raman, N. A. Choudhury, K. R. Priolkar, P. R. Sarode, S. Emura and R. Kumashiro, J. Electroanal. Chem. 563 (2004) 181.

[18] H. Yang, C. Coutanceau, J.-M. Leger, N. Alonso-Vante and C. Lamy, J. Electroanal. Chem. 576 (2005) 305.

[19] A.K. Shukla and R.K. Raman, *Annual Review of Materials Research* 33 (2004) 155

[20] U.A. Paulus, A. Wokaun, G.G. Scherer, T.J .Schmidt, V. Stamenkovic, V. Radmilovic, N.M. Markovic and P.N. Ross, J Phys. Chem. B 106 (2002) 4181.

[21] R.C. Koffi, C. Coutanceau, E. Garnier, J-M. Leger and C. Lamy, Electrochim. Acta 50 (2005) 4117.

[22] L. Xiong and A. Manthiram, J.Electrochem. Soc.152 (2005) A697.

[23] H. Uchida, H. Ozuka and M. Watanabe, Electrochim. Acta 47 (2002) 3629.

[24] T. Toda, H. Igarashi and M. Watanabe, J. Electroanal Chem. 460 (1999) 258.

[25] A.K. Shukla, R.K. Raman, N. A. Choudhury, K. R. Priolkar, P. R. Sarode, S. Emura and R. Kumashiro, J. Electroanal. Chem. 563 (2004) 181.

[26] C.F. Zinola, A.M. Castro Luna, W.E. Triaca and A.J. Arvia, *J. Applied Electrochem.* **24** (1994) 119.

[27] T. Toda, H. Igarashi, M. Uchida and M. Watanabe, *J. Electrochem. Soc*. **146** (1999) 3750.

[28] M. Pourbaix: "Atlas of Electrochemical Equilibria in Aqueous Solutions", Pergamon, New York, 1966

[29] P.A. Siminov and V.A. Likholobov, Catalysis and Electrocatalysis at Nanoparticle Surfaces (edited by A. Wieckowski, E. R. Savinova, C.G. Vayenas), M.Dekker Inc. (2003), pp 409.

[30] M. Watanabe and M. Uchida, S.Motoo, *J. Electroanal. Chem.* **229** (1987) 395.

[31] H.G. Petrow and R.G. Allen, U.S. Pattern 3,992,331 (1976).

[32] K. Kinoshita, *J.Electrochem. Soc.* **137** (1990) 845.

[33]H.G. Petrow, R.J. Allen, US Patent 3, 992, 331 (1976).

[34] V. Baglio, A.S. Aricò, A. Stassi, C. D'Urso, A. Di Blasi, A.M. Castro Luna, V. Antonucci, J. Power Sources 159 (2006) 900.

[35] A.S. Aricò, A.K. Shukla, K.M. el-Khatib, P. Cretì, V. Antonucci, J. Appl. Electrochem. 29 (1999) 671.

[36] Y. Xu, A. Ruban, M. Mavrikakis, J. Am. Chem. Soc. 126 (2004) 4717.

CHAPTER IV

ROTATING DISK ANALYSIS OF OXYGEN REDUCTION AT PT-FE CATALYST FOR LOW TEMPERATURE DIRECT METHANOL FUEL CELLS

IV. INTRODUCTION

In this part of the thesis, the aim is to present basic electrochemical investigation of the most promising carbon supported high metal loading Pt-Fe catalyst for the oxygen reduction in the presence of methanol. The oxygen reduction reaction properties, together with methanol tolerance characteristics, of Pt-Fe catalysts are examined and interpreted in the light of the structure, chemical and surface properties, as previously reported. The goal is to provide a contribution to the understanding of the catalytic properties for ORR of small nanostructured crystalline bimetallic Pt-M supported catalysts highly concentrated on the surface of a carbon black support.

The promising results obtained with a 60% Pt-Fe(5%)/C cathode catalyst have prompted us to examine, more in depth, the ORR activity of this catalyst by rotating disk technique. Thus, the catalyst was electrochemically characterized employing a thermostated standard three-electrode cell, the rotating disk electrode consisted of glassy carbon rod (0.125 cm^2 geometric area) covered by a thin layer of catalyst embedded in a Nafion polymer electrolyte film [1]. A Pt foil was used as counter electrode and a saturated calomel electrode as reference electrode, the latter separated from the working electrode section by a closed electrolyte bridge to avoid chloride contamination. The potentials are referred to that of the reversible hydrogen electrode (RHE). The electrolyte solution was 0.5 M H_2SO_4. The electrochemical experiments were conducted at different temperatures from 25 to 60 ^{0}C. Before working on ORR experiments, the disk composite electrode was cycled for 5 min at 0.1 V s^{-1} between 0.05 and 1.2 V in a N_2 purged sulfuric electrolyte solution to clean the surface. Subsequently, O_2 was bubbled in the solution and after 40 min, hydrodynamic current potential experiments were recorded by sweeping the potential from 1.0 V to 0.2 V at 5 mV s^{-1} under rotating rate between 200 to 1500 rpm. A 60% Pt/C was used as a reference to compare the results.

IV. 2 RESULTS AND DISCUSSION

The strategy adopted with the cathode catalysts was to synthesize formulations containing a high concentration of active catalytic phase on carbon whilst maintaining an appropriate particle size. The first approach concerned with the preparation of a 60% Pt/C catalyst with particle size around 3 nm.

The second approach concerned with the preparation of 60% Pt-5%Fe/C catalyst. The aim was to modify the Pt surface by transition metals, using a low temperature preparation route which does not significantly increase the particle size as in conventional Pt-M catalysts treated at 700-900 °C. The particle size remains quite small about 2.4 nm, and the structure-morphology investigations show a single fcc phase and a homogeneous distribution of fine metal particles on the support. The particle size distribution histograms for all catalysts are shown in Fig. IV-1. An unimodal particle size distribution is observed with particle sizes ranging from 1 to 5 nm.

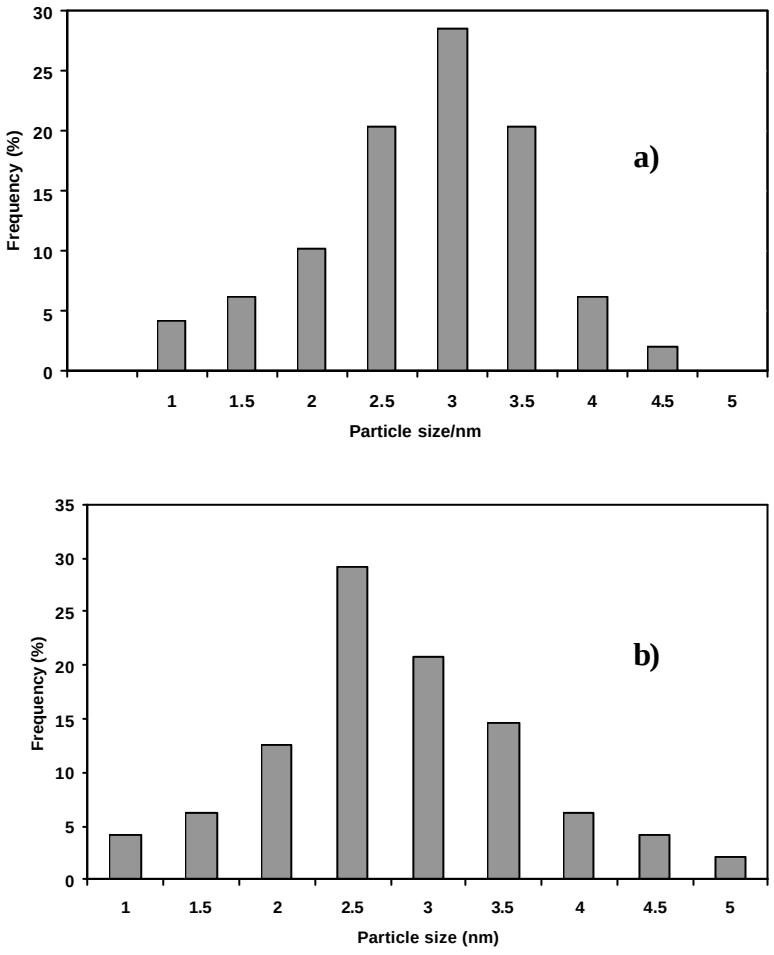

Fig. IV-1 Histograms of particle size distribution for (a) 60% Pt and (b) 60% Pt-Fe/C

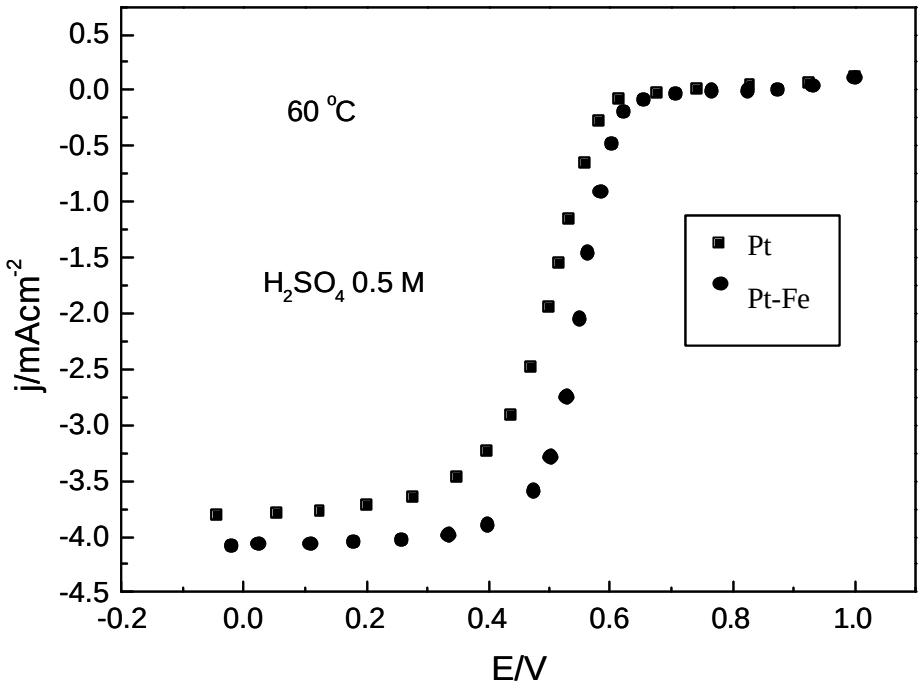

Fig IV-2 Polarization curves for ORR in 0.5 M H_2SO_4 at 60 °C on Pt/C and Pt-Fe/C cathode catalysts.

Polarization curves for ORR for different catalysts, namely Pt and Pt-Fe, in an oxygen saturated sulfuric solution at 60 ^{0}C and 1000 rpm are shown in Fig. IV-2. The onset potential for the ORR on Pt-Fe catalyst is shifted towards higher potential, indicating better catalytic characteristics of this alloy for ORR compared to the previous ones. Thus, due to the better performance, the attention was focused on Pt-Fe rather than on bare Pt. The influence of temperature change on the Pt-Fe performance is reported in Fig. IV-3. An enhancement of activation and mass transport properties is observed as the temperature is increased.

The electrochemical behaviour of Pt-Fe was also investigated in the presence of methanol in the acidic solution (Fig. IV-4) and compared to the Pt catalyst. Figure IV-5 shows the current density-potential profile for the ORR reaction on Pt and Pt-Fe catalysts with and without methanol in the solution at 1000 rpm. Both catalysts showed a decrease in performance in the presence of methanol. This effect is more noticeable with increasing methanol concentration (Fig. IV-4) or lowering of the rotation rate (not shown). With a methanol concentration of 0.05 M, a shift towards lower potentials was observed for both catalysts.

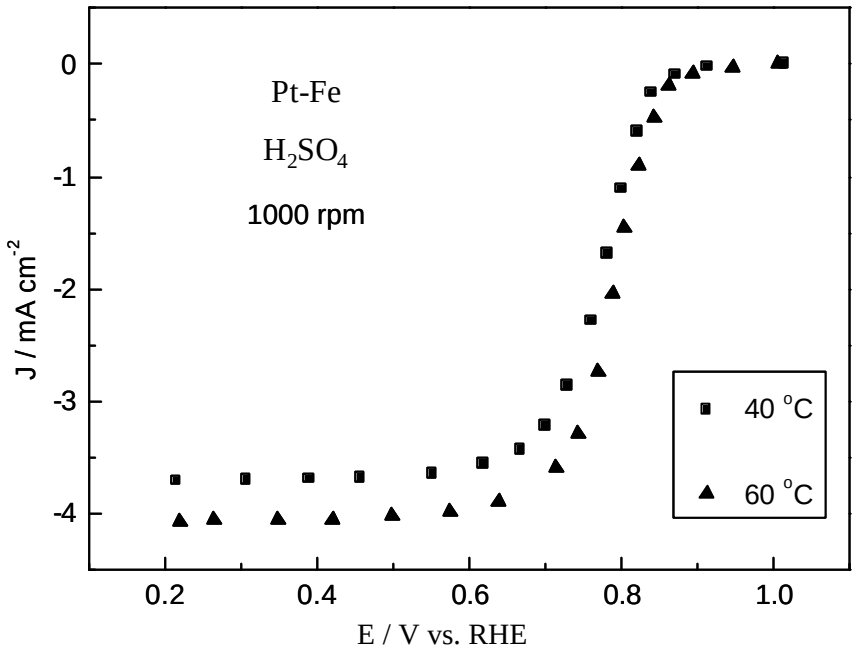

Fig. IV-3 Polarization curves for ORR in 0.5 M H_2SO_4 at 40°C and 60 °C on Pt-Fe/C cathode catalyst

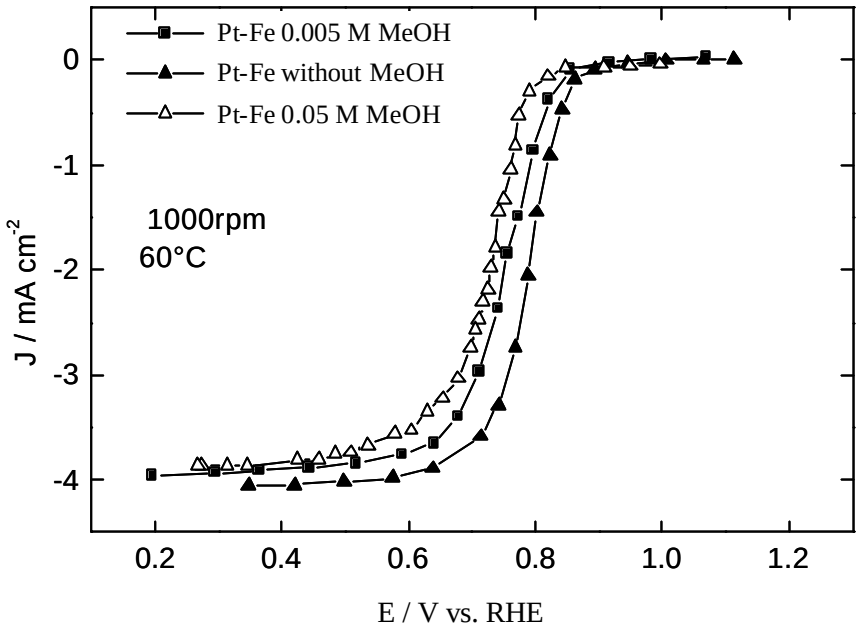

Fig. IV-4 Polarization curves for ORR in the presence of MeOH at different concentrations in 0.5 M H_2SO_4 at 60 °C on Pt-Fe/C cathode catalyst

However, the polarization curve on the Pt-Fe catalyst is less negatively shifted in the presence of methanol than that on Pt. This clearly indicates a promoting effect of the bimetallic catalyst in enhancing the ORR and a better tolerance to methanol. At potentials lower than 0.7 V, the performance of the Pt-Fe catalyst in the presence of methanol appears to be similar to that of Pt without alcohol. Similar methanol tolerance properties were found for Pt-Ni catalysts by Lamy and co-workers [2]. In order to get more insights on the mechanism, a Tafel analysis was carried out (see below).

Polarization curves for ORR on Pt-Fe electrode were measured at different rotation speeds (Fig. IV-6). The limiting current densities increase progressively as the rotation speed was increased, as expected. The curve obtained at 1000 rpm were selected to determine the electro-kinetic parameters.

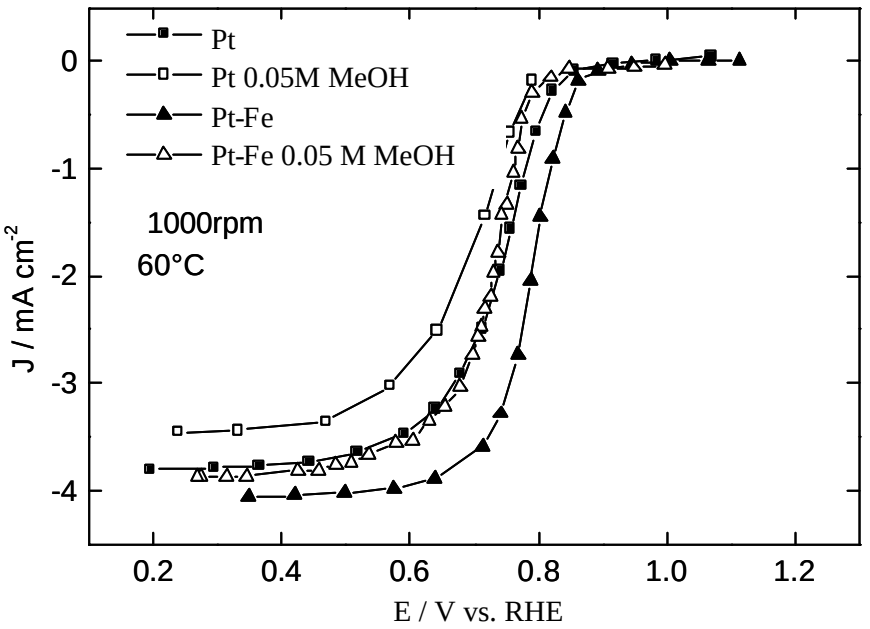

Fig. IV-5 Polarization curves for ORR at 1000 rpm and 60 °C on different catalysts in 0.5 M H_2SO_4 with and without methanol

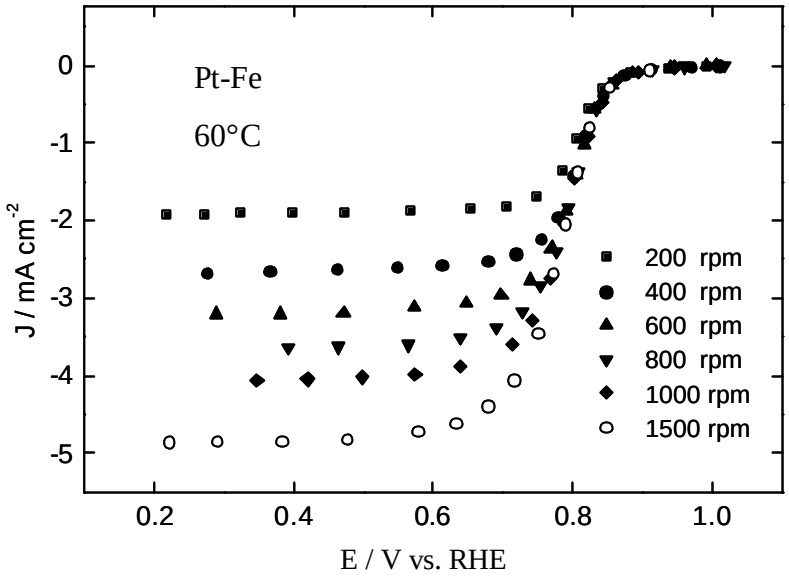

Fig IV-6 Polarization curves for ORR at 60 ^{0}C and different rotation speeds on the Pt-Fe catalyst in 0.5 M H_2SO_4 in pure oxygen.

Tafel plots for the oxygen reduction process were obtained after correction for the oxygen mass transport effects. The contribution of the film diffusion resistance to the measured current density is considered negligible [1]. At any cathode potential E, the current density J was calculated as $(J \cdot J_l)/(J_l - J)$, where J and J_l are the measured and the limiting current density, respectively. Assuming that the polarization behaviour after mass transport correction is mainly activation controlled, the corresponding Tafel plots (Fig. IV-7) in the range $0.6<E<0.9$ V were determined. Within the fitting error, the Tafel slope obtained at high potentials, ($E > 0.75$ V) on both Pt and Pt-Fe, was ca 0.065V decade^{-1}; and at low potentials ($E < 0.75$ V) ca 0.120 V decade^{-1}. It seems that there is no dependence of ORR mechanism on the composition and structural parameters of the catalysts. The exchange current densities for the Pt and Pt-Fe catalysts, determined in the region characterized by 0.120 V decade^{-1} Tafel slope, were $1.63 \cdot 10^{-5}$ mA cm^{-2} and $2.15 \cdot 10^{-4}$ mA cm^{-2} at 60°C, respectively. As suggested by Mukerjee [3], the presence of Fe in the binary Pt-Fe catalysts shifts the Pt-oxide formation towards higher potentials, favoring the ORR reaction, but it appears that there is no effect on the ORR rate determining step.

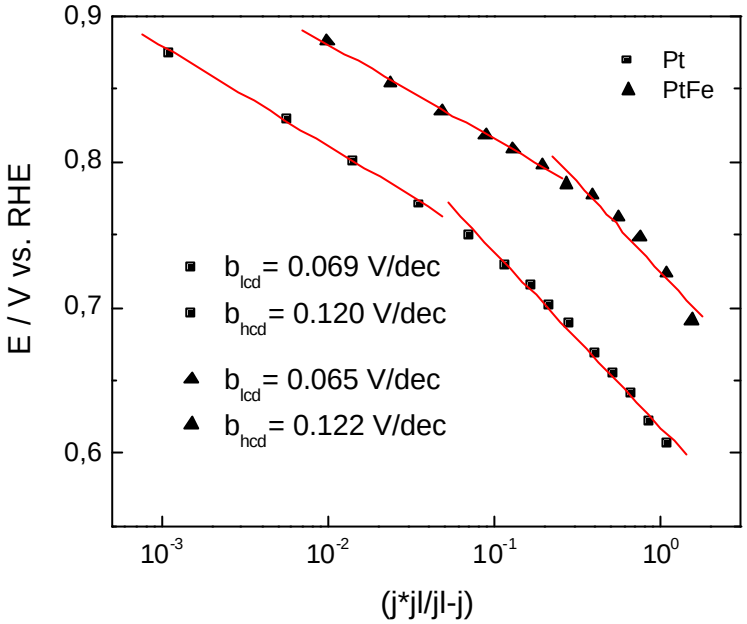

Fig. IV-7 Tafel plots for ORR in 0.5 M H_2SO_4 on different catalysts

The smaller particle size of the present Pt-Fe catalyst with respect to the Pt catalyst used for comparison could also be responsible of the enhanced activity. Recently, Leger et al.[4] have shown enhanced methanol tolerance for ORR of Pt-based catalysts as a function of particle size decrease. Furthermore, partial dissolution of iron into the electrolyte from poorly alloyed Pt-Fe catalysts may cause a slight increase in roughness and thus in the number of sites available for the reaction. This aspect was investigated by EDX analysis of the Pt-Fe catalyst before and after the operation in acidic solution (Fig. IV-8). This analysis confirms a decrease of Fe content in the catalyst of about 36% with respect to its initial concentration after polarization and cyclic voltammetry experiments in the sulfuric acid solution. This may cause an increase in roughness and surface area of Pt-Fe catalyst.

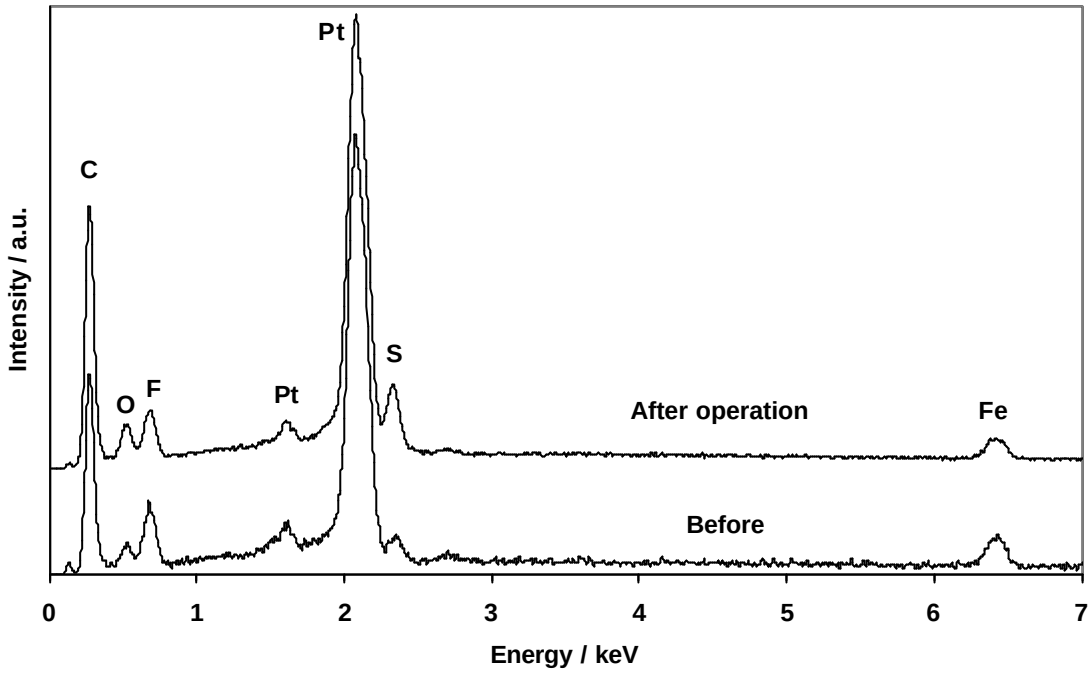

Fig. IV-8 EDX analysis of the Pt-Fe catalyst before and after operation.

IV. 3 CONCLUSION

A 60 wt% Pt-Fe/C catalyst with atomic composition of about Pt_3M_1 was prepared using a colloidal preparation procedure that has allowed synthesis of bimetallic catalysts with particle size less than 3 nm and with a suitable degree of alloying. The electrocatalytic behavior for ORR of these catalysts was investigated by employing the rotating disk technique and compared to that of a pure Pt/C catalyst with similar particle size. A promoting effect in enhancing the ORR was observed for the Pt-Fe alloy, compared to Pt catalyst, both with and without methanol in the oxygen-saturated electrolyte solution.

IV. 4 REFERENCES

[1] U.A. Paulus, T. J .Schmidt, H. A. Gasteiger and R. H. Behm, *J. Electroanal. Chem.* **495** (2001) 134.

[2] H. Yang, C. Coutanceau, J.-M. Leger, N. Alonso-Vante and C. Lamy, *J. Electroanal. Chem.* **576** (2005) 305.

[3] V. Murthi, R.C. Urian and S. Mukerjee, *J. Phys. Chem B* **108** (2004) 11011.

[4] F. Maillard, M. Martin, F. Gloaguen and J.-M. Leger, *Electrochim. Acta* **47** (2002) 3431.

CHAPTER V

OPTIMIZATION OF ELECTRODE PROPERTIES FOR LOW TEMPERATURE DMFC APPLICATIONS

V. INTRODUCTION

The aim of this study is to investigate DMFC MEAs with different electrode configurations varying in terms of gas diffusion layer and catalytic layer. In order to investigate the influence of these modifications on the cell performance, electrochemical characterizations were carried in a single cell of 5 cm^2 active area, for experiments under forced flow, and of 16 cm^2, for experiments under passive mode operation. The results were compared with the characteristics of a cell having a standard electrode configuration MEA.

Nowadays, direct methanol fuel cell electrodes mainly consist of gas diffusion electrodes similar to those used in H_2-fuelled proton exchange membrane fuel cells (PEFCs) [1-6]. Typically, such an electrode is made up of a first layer, which is a carbon cloth or paper. This is the conductive support onto which the gas diffusion layer and thereafter the catalytic layer are deposited. In most electrode configurations, 20 wt% Polytetrafluoroetylene (PTFE) and 80 wt% Carbon black form the gas diffusion layer, whereas a composite catalytic layer, consisting of carbon supported Pt or Pt alloy catalyst and Nafion ionomer is deposited onto the gas diffusion layer (GDL) [1, 5, 7, 8]. Such an electrode structure was originally developed for operation at about 80°C, since the development of DMFC for transportation was historically considered to provide the main perspectives for large-scale application of such devices. This electrode configuration in low temperature liquid-fuelled Direct Methanol Fuel Cells (DMFCs), finalized to the development of portable systems, suffers from mass-transport limitations mainly at the anode due to the low diffusion coefficient of methanol in water and the release of carbon dioxide gas bubbles [9, 10]. The influence of PTFE content in the anode diffusion layer on cell performance has been previously investigated for high temperature DMFCs. The optimal PTFE amount was found to be between 13 and 20 wt% [11]. Some recent studies have been addressed to replace the carbon cloth or carbon paper support with titanium net [10] to enhance mass transport. Alternatively, some attempts have been addressed to

enhance the morphology of the conventional electrode structure. As well known, a correlation between the amount of ionomer, in the catalytic layer, and catalyst porosity exists [18]. The ionomer content governs the hydrophobic and hydrophilic pore distribution in the catalyst layer. Hydrophilicity increases as a function of the Nafion content. DMFCs are generally operated with aqueous methanol solution at different concentrations. Therefore, in order to have a better reactant distribution, a good hydrophilicity is important for the anode side. On the other hand, hydrophobic pores have an important role for CO_2 removal from the catalytic layer. Thus, the aim of this work is to evaluate the effect of hydrophobic/hydrophilic property modifications of anode for operation in low temperature DMFCs. A similar investigation was also carried out for the cathode, where an appropriate balance of hydrophobic characteristics, necessary to avoid the flooding of the electrode, and triple-phase boundary can lead to significant amelioration of the performance.

V. 1 EXPERIMENTAL

A carbon supported Pt-Ru alloy (85 wt% Pt-Ru/Vulcan XC 72) catalyst was in-house prepared by a sulfite complex route [12, 13] and used for methanol oxidation. A 60 wt% Pt/Vulcan XC 72 was prepared in the same way and used at the cathode for the oxygen reduction reaction. Structural and morphological characteristics of both catalysts were investigated in a previous work [14]. The electrodes consisted of carbon cloth, diffusion and catalytic layers. Our standard electrode configuration was composed by a carbon cloth support, a gas-diffusion layer (GDL), composed by 80 wt% Acetylene Black and 20 wt% PTFE, and a catalytic layer consisting of 85 wt% catalyst and 15 wt% Nafion ionomer [5, 13]. The so-called standard composition was previously optimized for medium-high temperature operation (90-130°C) in the presence of high metal concentration catalysts [5]. As reported in Table V-1, the anodic structure was modified by introducing 10 wt% Nafion ionomer in the GDL instead of PTFE, thus forming a composite diffusion layer composed of 90% Carbon and 10% Nafion, in order to make the GDL more hydrophilic. In MEA 2, the catalytic layer was composed by a "standard" configuration, i.e. composite catalyst/Nafion (85 wt%/15 wt%) [5]; in MEA 1, the Nafion content was lowered to 5 wt%. Details of the cathode configuration are reported in Table V-2. In a first approach, PTFE was added to a slurry composed by the catalyst and water; the resulting paste was spread onto the conventional diffusion layer. After sintering at 350°C, a 33 wt% Nafion

with respect to the catalyst amount was spread on the surface (MEA 3). Another attempt was performed by mixing catalyst, PTFE and Nafion, without any sintering process to avoid the degradation of Nafion (MEA 4). A Pt loading of 4 ± 0.2 mg cm^{-2} was used for both anodes and cathodes. A Nafion 117 membrane was employed as electrolyte in all experiments. Membrane-electrode assemblies (MEAs) were formed by a hot-pressing procedure [5] and subsequently installed in a fuel cell test fixture of 5 cm^2 active area, for experiments under forced flow, and of 16 cm^2, for experiments under passive mode operation. The first one was connected to a test station including an HP6060B electronic load. For single cell polarization experiments, aqueous methanol (1 M) was pre-heated at the same temperature of the cell and fed to the anode chamber of the DMFC through a peristaltic pump; dry air, pre-heated at the same temperature of the cell, was fed to the cathode. Atmospheric pressure in the anode and cathode compartments was used for all experiments. Reactant flow rates were 2 ml min^{-1} and 350 ml min^{-1} for methanol/water mixture and air stream, respectively. The second one was an air-breathing housing for the cathode with a reservoir for the methanol solution at the anode. Different methanol concentrations were fed (from 0.5 M up to 20 wt% Methanol solution) operating under passive mode at room temperature (about 20°C). Single cell performances were investigated by steady-state polarization measurements.

V. 2 RESULTS AND DISCUSSION

In the first step of our analysis, the attention was focused on the operation under a forced flow of reactants. In particular, the investigation was addressed on the anode configuration, using a standard cathode composed by a carbon cloth support, a GDL, composed by 80 wt% Acetylene Black and 20 wt% PTFE, and a catalytic layer composed by 85 wt% catalyst and 15 wt% Nafion ionomer. As reported in Table V-1, the anodic structure was modified as follows: in MEA 2 the catalytic layer was composed by the standard composition of the composite catalyst/Nafion (85/15); in MEA 1, Nafion content was lowered at 5 wt%. The MEAs equipped with these two anode electrodes were electrochemically characterized in a 5 cm^2 single cell and compared to a standard MEA, containing our conventional electrode configurations. Polarization and power density curves at 30 and 60°C are reported in Figs. V-1 and V-2.

Table V-1. Composition of MEAs with different anodic characteristics

		Standard MEA	MEA 1	MEA 2
Anode	Diffusion layer	80% carbon 20% PTFE	90% carbon 10% Nafion	90% carbon 10% Nafion
	Catalytic layer	85% catalyst 15% Nafion	95% catalyst 5% Nafion	85% catalyst 15% Nafion
Cathode	Diffusion layer	80% carbon 20% PTFE	80% carbon 20% PTFE	80% carbon 20% PTFE
	Catalytic layer	85% catalyst 15% Nafion	85% catalyst 15% Nafion	85% catalyst 15% Nafion

Table V-2. Composition of MEAs with different cathodic characteristics.

		Standard MEA	MEA 3	MEA 4
Anode	Diffusion layer	80% carbon 20% PTFE	80% carbon 20% PTFE	80% carbon 20% PTFE
	Catalytic layer	85% catalyst 15% Nafion	85% catalyst 15% Nafion	85% catalyst 15% Nafion
Cathode	Diffusion layer	80% carbon 20% PTFE	80% carbon 20% PTFE	80% carbon 20% PTFE
	Catalytic layer	85% catalyst 15% Nafion	80% catalyst 20% PTFE 33% Nafion *(with respect to catalyst) on the surface of the electrode*	90% catalyst 10% PTFE 15% Nafion *(with respect to catalyst) in the slurry*

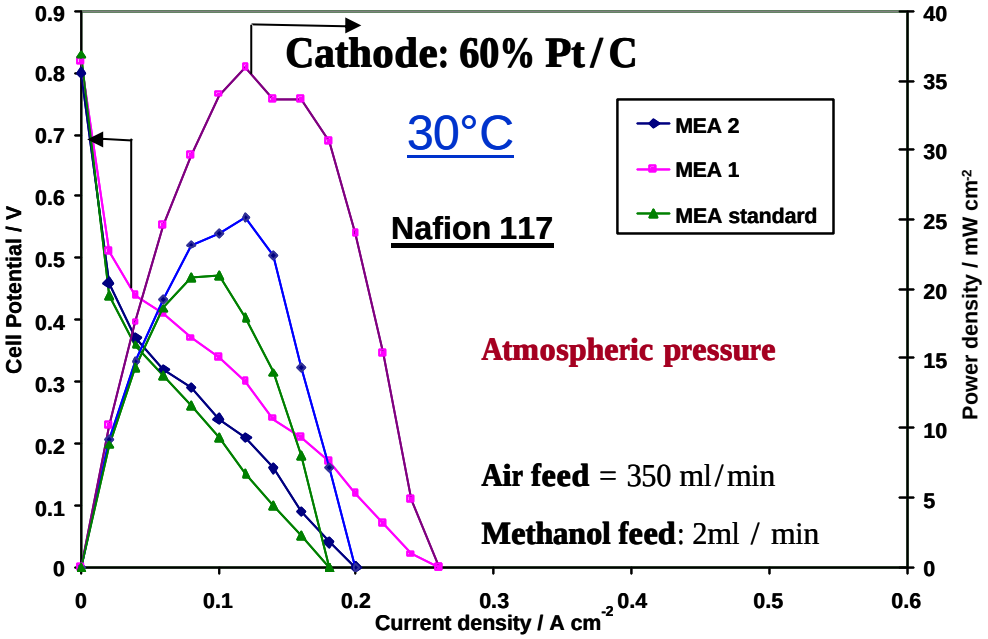

Fig. V-1 Polarization and power density curves at 30°C

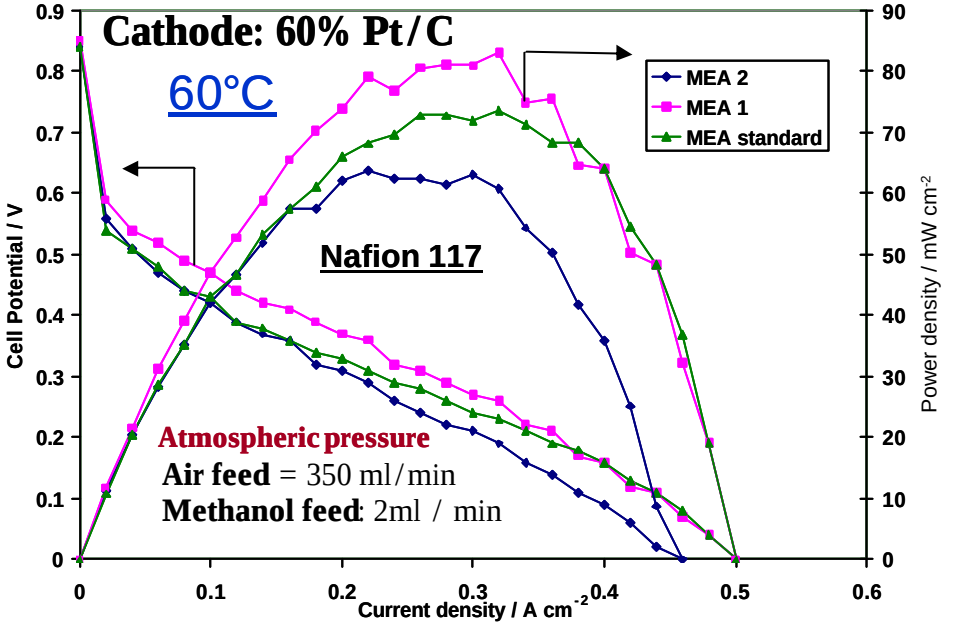

Fig.V-2 Polarization and power density curves at 60°C

Figs.V-1-2 show that the cell equipped with MEA 1 is characterized by lower potential losses in activation, ohmic and mass transport regions than the other MEAs. This indicates good performance both in terms of power density, about 36 and 83 mW/cm^2, and in terms of short circuit current density, about 0.26 and 0.5 A cm^{-2}, at 30 and 60°C, respectively. Table V-3 reports in detail the electrochemical results.

Table V-3. Summary of the main electrochemical results for MEAs characterised by different anodic compositions

Cell	Maximum Power Density (mW cm-2) Obar		Cell Voltage (V) at 30°C			Cell Voltage (V) at 60°C			Cell Resistance (Ohm cm2)	
	30 °C	60°C	50mA/ cm2	100mA/ cm2	200 mA/ cm2	50mA/ cm2	100mA/ cm2	200 mA/ cm2	30 °C	60 °C
MEA ST.	21	67,6	0.36	0.21		0.51	0.44	0.32	0.2	0.1
MEA 1	38,4	83,2	0.44	0.34	0.17	0.54	0.47	0.37	0.175	0.13
MEA 2	25,2	63	0.37	0.24	NR	0.51	0.42	0.31	0.25	0.15

The lower potential losses in the activation region for MEA 1 compared to the other two MEAs (MEA 2 and MEA 3) could be related to higher local pH due to the lower Nafion content in the catalytic layer. By analyzing the stoichiometry of methanol electro-oxidation process there is a release of protons from the molecule, thus, the anodic process is slightly shifted towards lower potential versus NHE by an increase of the local pH. It is well known that the methanol oxidation is accelerated in alkaline environment [15-17]. Yet, the use of alkaline electrolytes is hindered by the reaction with CO_2 forming carbonates. On the other hand, a compromise between proton conductivity and reaction rate is necessary to optimize the performance. The higher short circuit current density is due to the higher hydrophilic characteristics of the gas diffusion layer on the anode side. This favours reactant diffusion towards the reaction sites. On the contrary, CO_2 removal is favoured by hydrophobic pathways. Yet, an excess of hydrophobic properties for the diffusion layer, as in the standard MEA, does not significantly appear to favour the CO_2 removal or, possibly, this is not the rate determining step for the mass transport process at low temperatures. It appears that mass transport properties are dominant by methanol transport to catalytic sites. Possibly, the CO_2 removal is assisted by the forced convection process caused by the liquid pump. It may be rate determining in the passive mode operation [18-19], which will be discussed later in the text.

Further investigations were carried out by changing the standard cathode configuration, in order to study the effects of these modifications on the oxygen electro-reduction. Tests were carried out by using a standard anode configuration as reported in Table V-2 under forced flow operation. The MEAs based on these modified cathode electrodes (MEAs 3 and 4, see Table V-2) were electrochemically characterised in a single cell and compared to a standard MEA (Figs. V-3 and V-4).

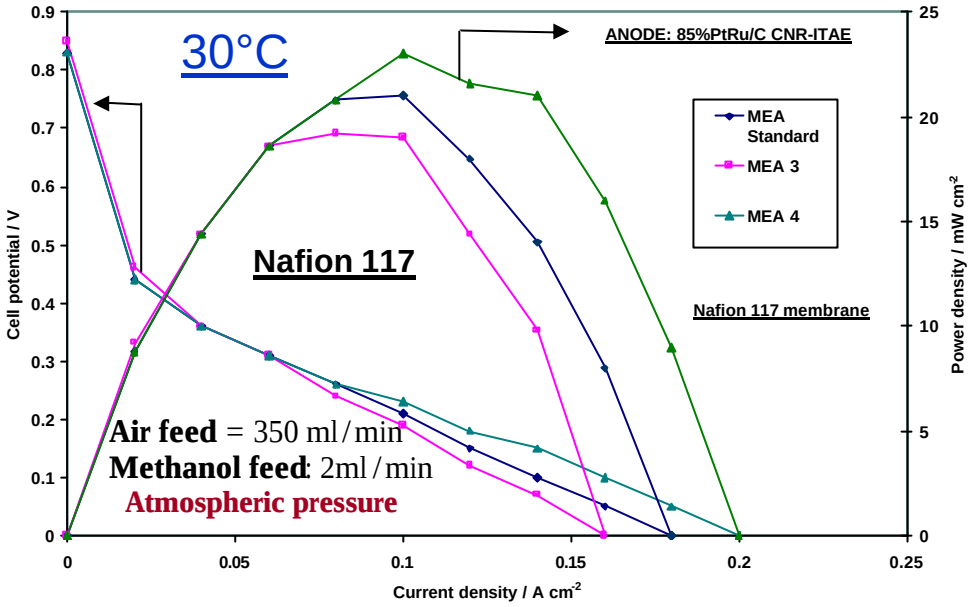

Fig. V-3 Polarization and power density curves at 30 °C

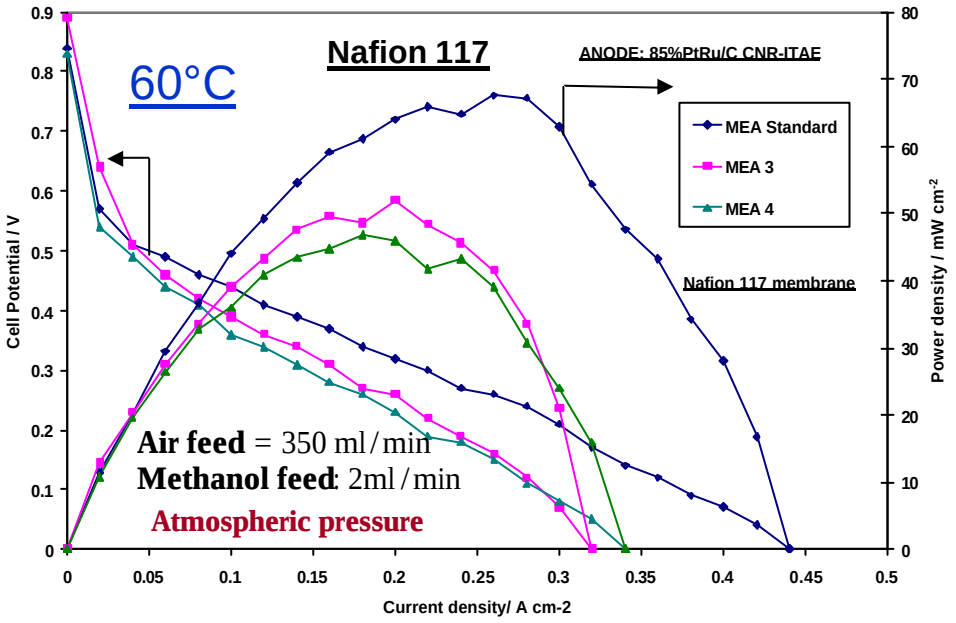

Fig. V-4 Polarization and power density curves at 60 °C

Figs. V-3 and V-4 show a comparison of the three different MEA configurations at 30 and 60°C. A slight increase of performance in the activation region for the MEA 3 is observed at 30°C. This effect is due to the electrode sintering at 350°C that enhances the hydrophobic characteristics of the PTFE allowing a better oxygen solubility in the catalytic layer at the three-phase boundary. However, MEA 3, due to this extremely high content of insulating hydrophobic component, shows evident potential losses in the ohmic region and consequently a decrease in the cell performance is observed. It is possible to observe better performance for the cell equipped with MEA 4 having a 10% of PTFE in the catalytic layer. This percentage of PTFE allows a good gas diffusion without causing any significant losses in the ohmic region. The maximum power density at 30°C was obtained using this MEA 4 and it was about 23 mW/cm^2. At temperatures higher than 30°C, flooding phenomena should be less significant. Therefore, a higher content of hydrophobic component, in the electrodic layer, does not appear to be necessary. A confirmation of this conjecture is provided by a comparison of the different MEAs at 60°C. The standard MEA shows better performance and a maximum power density of about 67.6 mW/cm^2 was recorded (Table V-4).

Table V-4. Summary of the main electrochemical results for MEAs characterised by different cathodic compositions

Cell	Maximum Power density mW cm-2 at 0 bar rel.		Cell Voltage (V) at 30°C			Cell Voltage (V) at 60°C			Cell Resistance Ohm cm2	
	30 °C	60°C	50mA/ cm2	100mA/ cm2	200 mA/ cm2	50mA/ cm2	100mA/ cm2	200 mA/ cm2	30 °C	60 °C
MEA ST.	21	67,6	0.36	0.21	NR	0.51	0.44	0.32	0.2	0.1
MEA 3	19,2	52	0.36	0.19	NR	0.51	0.39	0.26	0.4	0.3
MEA 4	23	46,8	0.36	0.23	NR	0.49	0.36	0.23	0.325	0.215

The best anode configuration (MEA 1) and the best cathode structure for low temperature operation, 30°C, (MEA 4) were used, together with Nafion 117 as electrolyte, for the investigation of an air breathing system operating at room temperature under passive mode. This MEA, which is called MEA 5, was investigated and compared to the standard MEA under the same operating conditions (room temperature, same housing and fuel cell test station, passive mode operation). Methanol solutions at different

concentrations (0.5 M, 1 M, 2 M and 20 wt.% Methanol in water) were added to the anodic reservoir and analysed in this DMFC device both with MEA 5 and standard MEA. The results are reported in Fig. V-5 a, b, c, d.

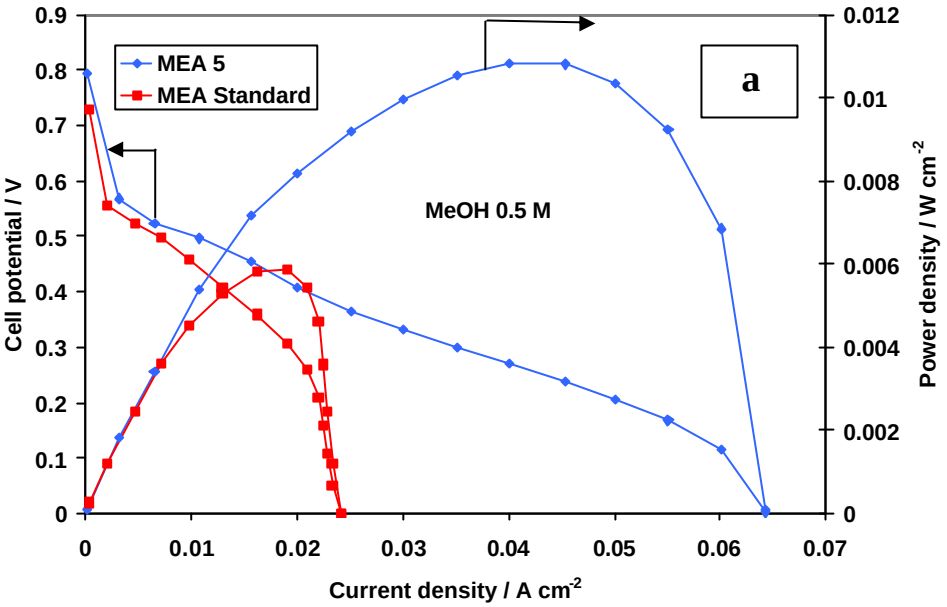

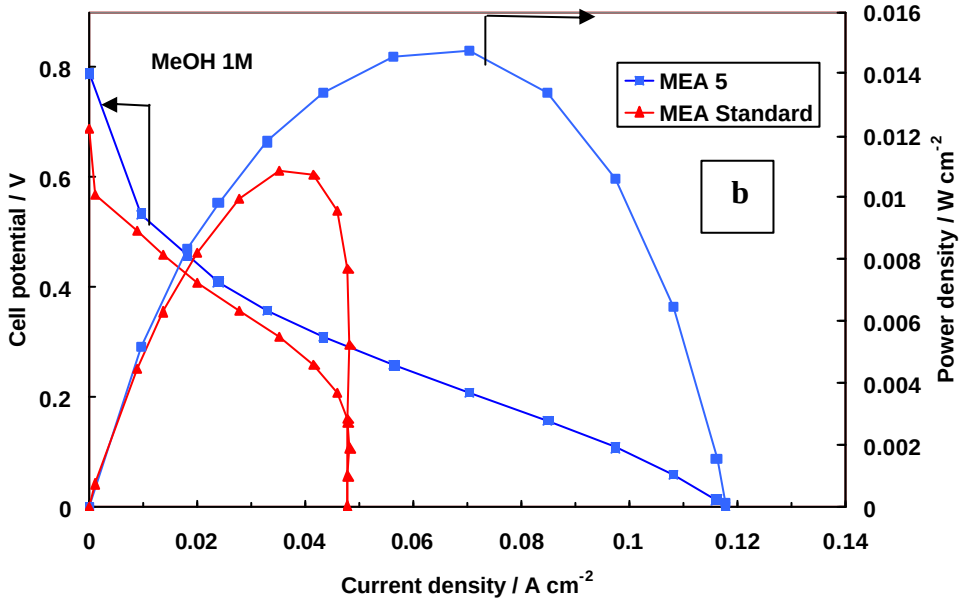

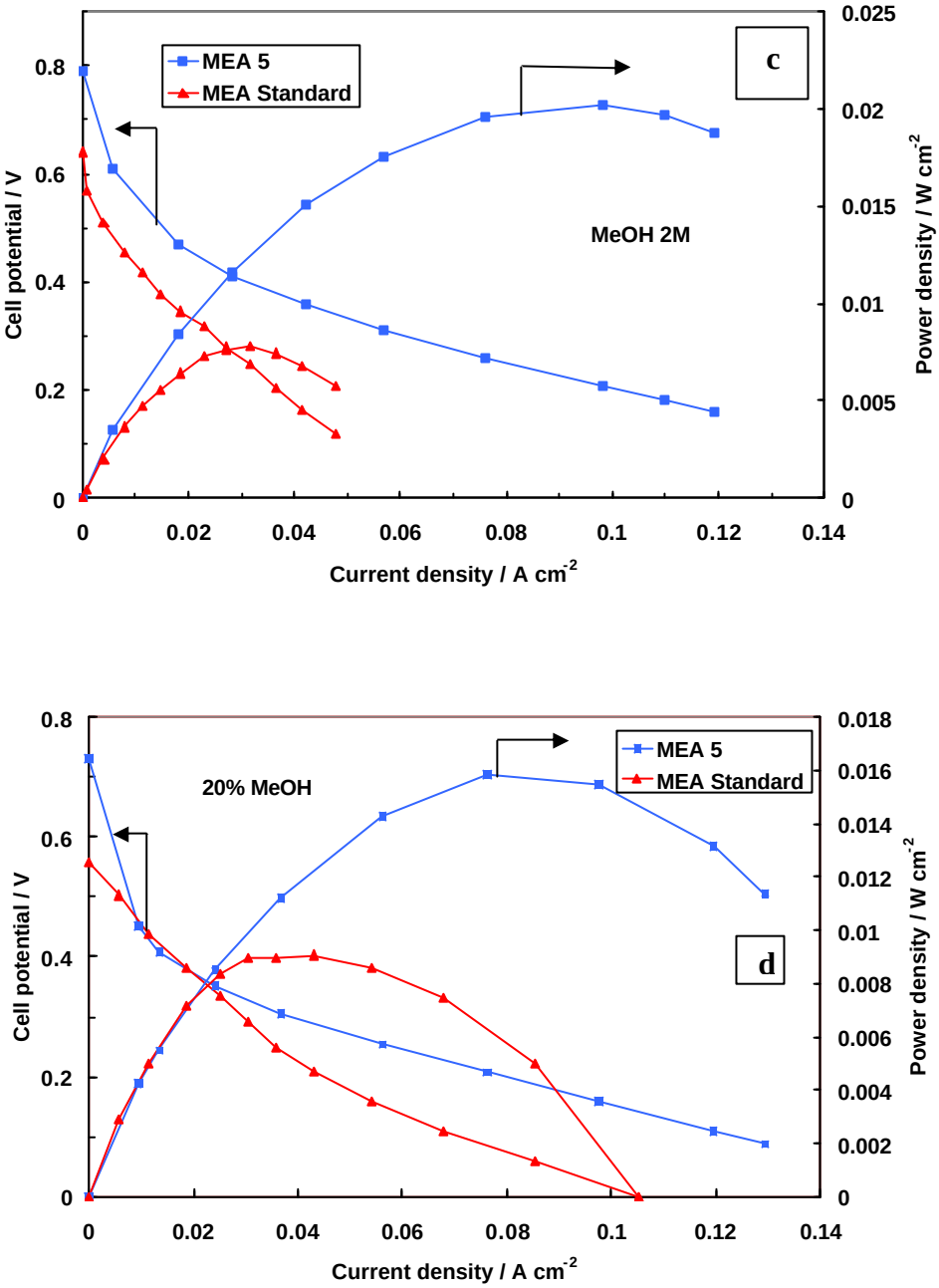

Fig V-5 Polarization and Power density curves at different methanol concentrations: a) 0.5 M, b) 1 M, c) 2 M, d)20wt%.

The MEA 5 is performing better than standard MEA for all methanol concentrations. The maximum power density of 20 mW/cm² is achieved with 2 M methanol. Such better performance is due to proper combination of hydrophilic properties of the anode and hydrophobic properties of the cathode.

At low methanol concentrations (0.5 M) a significant increase of performance is obtained for the advanced MEA 5 especially at high current density. This is due to better

mass transport properties. Whereas with 2 M methanol concentration the gain in performance is recorded in the overall current density range. This results from enhancement of the reaction process in both activation and mass transport control region. In the presence of 20 wt% methanol, the loss in performance in the activation region for the MEA 5 is quite significant due to the large methanol cross-over; yet, the maximum power density is still superior than that with standard MEA.

V. 3 CONCLUSIONS

The present analysis was addressed to evaluate separately the effect of modification of hydrophilic/hydrophobic properties of anode and cathode for operation in low temperature DMFCs. It was found that, under above conditions, CO_2 removal is not critical compared to methanol transport to the catalytic sites. Thus, an enhancement of anode hydrophilicity is favourable for the process. For what concerns the cathode, the increase of hydrophobicity, to counteract the effect of flooding, is appropriate only for low temperature operation (30°C). At higher temperatures an increase of ohmic resistance occurs as a consequence of the increase of hydrophobicity for the layer. The appropriate combination of anode and cathode properties as well as a tailoring of electrode characteristics for air breathing system operating at room temperature under passive mode were also investigated. Under these conditions, the MEA equipped with a more hydrophilic anode and more hydrophobic cathode has shown better mass transport characteristics and thus a higher power density (20 mW/cm^2) with respect to a MEA standard.

V. 4 REFERENCES

[1] X. Ren, M.S. Wilson and S. Gottesfeld, *J. Electrochem. Soc.* **143** (1996) L12.

[2] C. Lamy, S. Rousseau, E.M. Belgsir, C. Coutanceau and J.-M. Leger, *Electrochim. Acta* **49** (2004) 3901.

[3] W.J. Zhou, B. Zhou, W.Z. Li, Z.H. Zhou, S.Q. Song, G.Q. Sun, Q. Xin, S. Douvartzides, M. Goula and P. Tsiakaras, *J. Power Sources* **126** (2004) 16.

[4] A.K. Shukla, P.A. Christensen, A.J. Dickinson and A. Hamnett, *J. Power Sources* **76** (1998) 54.

[5] A.S. Aricò, A.K. Shukla, K.M. el-Khatib, P. Cretì and V. Antonucci, *J. Appl. Electrochem.* **29** (1999) 671.

[6] A. Oedegaard, C. Hebling, A. Schmitz, S. Moller-Holst and R. Tunold, *J. Power Sources* **127** (2004) 187.

[7] V. Baglio, A.S. Aricò, A. Stassi, C. D'Urso, A. Di Blasi, A.M. Castro Luna and V. Antonucci, *J. Power Sources* **159** (2006) 900.

[8] S.C. Thomas, X. Ren and S. Gottesfeld, *J. Electrochem. Soc.* **146** (1999) 4354.

[9] H. Yang, T.S. Zhao and Q. Ye, *J. Power Sources* **139** (2005) 79.

[10] Z.-G. Shao, F. Zhu, W.-F. Lin, P.A. Christensen, H. Zhang and B. Yi, *J. Electrochem. Soc.* **153** (2006) A1575.

[11] K. Scott, W.M. Taama and P. Argyropoulos, *J. Appl. Electrochem.* **28** (1998) 1389.

[12] H.G. Petrow and R.J. Allen, *US Patent* 3,992,331 (1976).

[13] A.S. Aricò, V. Baglio, A. Di Blasi, E. Modica, P.L. Antonucci and V. Antonucci, *J. Electroanal. Chem.* **557** (2003) 167.

[14] V. Baglio, A. Di Blasi, E. Modica, P. Cretì, V. Antonucci and A.S. Aricò, *J. New Mat. Electrochem. Sys.* **9** (2006) 41.

[15] K.-F. Zhang, D.-J. Guo, X. Liu, J. Li, H.-L. Li and Z.-X. Su, *J. Power Sources* **162** (2006) 1077.

[16] D.-J. Guo and H.-L. Li, *Carbon* **43** (2005) 1259.

[17] J.-M. Leger, *J. Appl. Electrochem.* **31** (2001) 767.

[18] H.K. Kim, *J. Power Sources* **162** (2006) 1232.

[19] G.Q. Lu and C.Y. Wang, *J. Power Sources* **134** (2004) 33.

CONCLUSIONS

The research activity of this thesis was addressed towards the development of low temperatures DMFC for portable applications. Different issues were studied and discussed in this thesis. They are summarized as follows.

The influence of noble metal loading and catalyst utilization on the electrochemical behaviour of low temperature (30-60°C) DMFCs was investigated by steady-state polarizations and adsorbed methanolic residues stripping voltammetry. From these analyses, 5 $mg \cdot cm^{-2}$ seems to be the most suitable Pt loading at the cathode for low temperature DMFC application. Whereas, 2 $mg \cdot cm^{-2}$ Pt loading at the anode is sufficient to achieve suitable performance. The maximum power density increased from 30 to 75 mW cm^{-2} at 60°C passing from 1 to 5 $mg \cdot cm^{-2}$ Pt loading on both anode and cathode at ambient pressure, whereas only a slight increase was observed with 10 $mg \cdot cm^{-2}$, due to the decrease of catalyst utilisation.

A preparation procedure was developed to modify the Pt catalysts with transition metals. A moderate degree of alloying was obtained with Pt-Fe/C cathode catalyst by using this low temperature preparation route. Whereas, the degree of alloying was slightly larger for Pt-Co/C and significantly larger for Pt-Cu/C compared to Pt-Fe by using the same procedure. High surface area carbon supported bimetallic Pt-Co, Pt-Cu and Pt-Fe catalysts were investigated for the oxygen electro-reduction process in low temperature direct methanol fuel cells (60 °C) and compared to Pt/C catalysts. Adsorbed methanolic residues stripping analysis showed a better methanol tolerance and an enhanced activity towards oxygen reduction in the case of the Pt-Fe system. An improvement of the DMFC single cell performance was also observed in the presence of Pt-Fe catalysts. The better performance obtained from the electrochemical analysis carried out on a 60% Pt Fe(5%)/C has led to examine, more in depth, the ORR activity for the catalyst by rotating disk technique and compared to that of a pure Pt/C catalyst with similar particle size. A promoting effect in enhancing the ORR was observed for the Pt-Fe alloy, compare to Pt catalyst, both with and without methanol in oxygen-saturated electrolyte solution.

MEAs with different electrode configurations varing in terms of gas diffusion layer and catalytic layer were investigated. This study was carried out in order to evaluate separately

the effect of modification of hydrophilic/hydrophobic properties of anode and cathode both under forced convection flow and passive mode operations.

It was found that a high hydrophilic characteristic on GDL, on the anode side, favours significantly a higher reactant distribution rate on the reaction pores. Both under forced convection flow and passive mode operation, CO_2 removal is not critical compared to methanol transport to the catalytic sites. Moreover, for what concern the cathode, the increase of hydrophobicity to counteract the effect of flooding, is appropriate only for low temperatures operation (30°C). At higher temperatures an increase of ohmic resistance occurs as consequence of the increase of hydrophobicity for the layer.

In order to have an information about a condition similar to a practical DMFC for portable application, tests under passive mode operations were carried out. The best results were achieved by using a hydrophilic anode and hydrophobic cathode. This MEA has shown better mass transport characteristics and thus a higher power density (20 mW/cm^2) with respect to a MEA standard.